A Consolidated Model for UHF/SHF Telecommunication Links Between Earth and Synchronous Satellites

H.T. Dougherty

TABLE OF CONTENTS

LIST OF FIGURES

LIST OF TABLES

A CONSOLIDATED MODEL FOR UHF/SHF TELECOMMUNICATION LINKS BETWEEN EARTH AND SYNCHRONOUS SATELLITES

H. T. Dougherty*

The radio wave propagation path between an earth station and a synchronous satellite is described by engineering-type formulas which consolidate all of the known external elements significant for system performance. This UHF/SHF consolidated model, adaptable for subsequent updating, includes state-of-the-art estimates of noise, attenuation, depolarization, and turbulence. The role of system geometry in signal depolarization is presented and the basis for the evaluation of linear versus circular polarization is developed. The conventional figures of merit are included; the determination of service fields (desired signal levels) and potential interference fields (undesired signal levels) are described. The application of the formulas and graphs given in the text are illustrated by numerical examples; their associated derivations are either referenced or covered in the appendices.

Key Words: atmospheric attenuation; frequency allocation; depolarization; frequency sharing; interference fields; propagational effects; service fields; SHF; slant path; UHF

1. INTRODUCTION

The propagation paths between earth stations and synchronous satellites for either system design or regulatory purposes require a modeling which incorporates all known significant elements. To meet this need for a consolidated model capable of being subsequently updated or adapted to related special cases, this report proposes an Institute for Telecommunication Sciences (ITS) UHF/SHF model (300 to 30,000 MHz or, as preferred here, 0.3 to 30 GHz).

From the point of view of radio wave propagational effects, a model for earth-space systems both resembles and markedly differs from that of terrestrial systems. The resemblance is to be expected, since the purposes and techniques of telecommunications are the same. The differences result largely from the different geometry and environment involved. For example, earth-space systems are normally radio-line-of-sight (RLOS), but with only one terminal and a small portion of its propagation path immersed in the terrestrial environment. While this generally frees earth-satellite systems from many terrestrial system limitations, it also introduces some new limitations peculiar to satellite systems.

---

* The author is with the U. S. Department of Commerce, National Telecommunications and Information Administration, Institute for Telecommunication Sciences, Boulder, Colorado 80303.

1.1 A Reference System Parameter

One of the similarities to terrestrial systems at UHF and SHF is the availability of the reference free-space loss. An earth-satellite system involves radio wave propagation between two terminals for which the propagation loss, L in decibels, may be given in terms of the equivalent free-space basic transmission loss, L_{bo} in decibels, plus add-on terms that reflect the additional losses attributable to the atmosphere and system geometry. The free-space transmission loss is

$$L_o = 10 \log_{10} \frac{p_T}{p_R} = P_T - P_R = L_{bo} - G_T - G_R - 20 \log_{10} \delta_o \quad dB \tag{1}$$

$$= 92.45 + 20 \log_{10} f + 20 \log_{10} r - G_T - G_R - 20 \log_{10} \delta_o \quad dB \tag{2}$$

Here, p_T is the transmitter power in watts; $P_T = 10 \log_{10} p_T$ dBW;

p_R is the received power in watts; $P_R = 10 \log_{10} p_R$ dBW;

G_T is the transmitting antenna gain in the direction of the propagation path, less line and radome losses, in dBi (decibels above that for an isotropic antenna);

G_R is the receiving antenna gain in the direction of arrival of the propagation path, less line and radome losses, in dBi (decibels above that for an isotropic antenna);

f is the transmission frequency in gigahertz;

r is the propagation path length or range in kilometers; and

δ_o is the loss factor due to the polarization discrepancy between transmitting and receiving antennas, but exclusive of atmospheric and antenna effects.

L_{bo} is the equivalent free-space <u>basic</u> transmission loss in decibels given explicitly by the first three terms of (2) above [Rice et al., 1966].

Note that the constant is 92.45 dB when the frequency f is in gigahertz, as in (2) above. A possibly more familiar value is the 32.45 dB, appropriate when the frequency is expressed in megahertz.

The term δ_o is explained more fully later in the text, but here we note that for terrestrial systems δ_o would commonly be unity so that this term has not appeared previously in association with free-space losses.

1.2 Organization of this Report

Section 2 of this report describes the basic geometry of earth/satellite systems and the associated parameters (elevation angle, range, etc.) required to specify the propagational effects. Section 3 introduces the environmental effects that are significant for frequency allocation or system design; i.e., the determination of the system's service field (desired signal level). Section 4 describes the conventional figures of merit.

Section 5 describes the geometrical and environmental conditions that are significant for frequency sharing; i.e., the determination of potential interference fields (undesired signals). Several appendices are added so as to detail the data that are summarized in the text.

The emphasis in this report is upon engineering-type formulations which systematically include state-of-the-art estimates. Subsequently, more reliable estimations may be included as continuing investigations and operational experience formulate them.

2.0 THE EARTH/SATELLITE GEOMETRY

For an earth/space system, the space terminal or satellite will orbit about the earth in a trajectory that may generally be approximated as an ellipse. As detailed in Appendix A, the ellipse will have one of its foci at the earth's center of gravity, and the radial distance from that center to the satellite may be expressed as $\rho(\psi)$, a function of the orbiting angle ψ measured from perigee (Appendix Figure A1). For the systems engineer, a more useful parameter is the range appropriate to (1) and (2). That range may be expressed as simply r in kilometers or more generally as a function $r(\varepsilon,A)$ of the elevation angle (ε) to the satellite(s) and the azimuth (A) to the subsatellite point (SS), measured from the earth station (ES).

2.1 The Earth/Synchronous Satellite Parameters

For a synchronous satellite (i.e., in a near-circular, near-equatorial orbit of period T = 24 hr), the satellite will appear to move in a figure-eight-like pattern about a stationary point in the sky which projects as a fixed subsatellite point (SS) on the earth's equator. There is an associated fixed geometry as illustrated by the insert drawing on Figure 1. When the orbit of the synchronous satellite becomes circular in the equatorial plane, the satellite is geostationary and positioned by the four parameters $(Z,r,\varepsilon,$ and $\phi)$ of Figure 1. Note that:

3
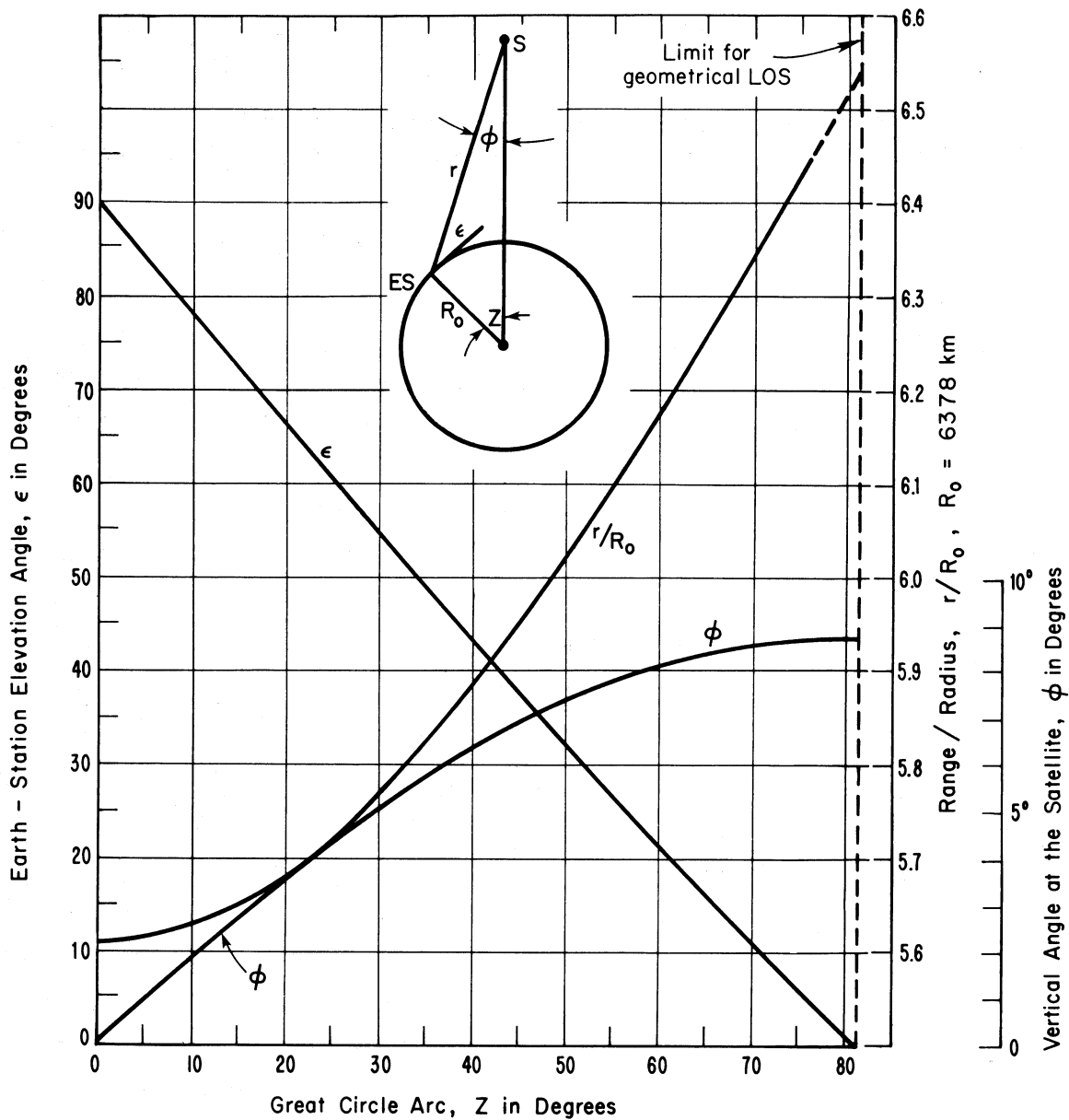
Figure 1. The four earth/satellite basic path parameters (z, r, ε, φ) related for a synchronous satellite. The minumum and maximum values of r would be 35,785 km (r/R$_0$ = 5.6107) and 41,678 km (r/R$_0$ = 6.53465).

Z   is the great-circle arc between the earth station (ES) and the sub-
    satellite point (SS) and may be given either in degrees of arc and
    as a central angle or as an arc length in kilometers, 111.32 km per
    degree of subtended central angle (see Figure 1 inset);

r   is the slant-path range in kilometers between the earth station
    and the satellite (ES to S);

ε is the propagation path elevation angle at the earth station, meas-
    ured in degrees above the local tangent at ES; and

ϕ is the acute angle measured in degrees from the vertical (radial)
    at the satellite (S).

These four propagation path parameters $(z, r, \varepsilon, \phi)$ constitute a set; given one, the
other three are determined. This is illustrated in Figure 1 and detailed in
Appendix A [Yeh, 1972; ITU, 1979].

Normally a synchronous satellite is positioned in terms of the longitude of its
subsatellite point (SS) on the equator; then the earth station (ES) can be located
by its:

L   the degree of latitude, north (L>0) or south (L<0);

$\delta\ell$ the degrees of longitude that ES lies east ($\delta\ell$>0) or west ($\delta\ell$ <0)
    of the SS point;

Z   the degrees of great-circle arc between ES and SS;

A   the degrees of azimuth from ES to SS; and

B   the degrees of back-azimuth from SS to ES.

These five positional parameters (L, $\delta\ell$, Z, A, and B) constitute a set; knowing
the value of any two, the values of the other three are determined, as detailed in
Appendix A. Figure 2 illustrates both sets of parameters L, $\delta\ell$, Z, A, B, r, ε, ϕ.

Figure 3 illustrates the relationship between L, $\delta\ell$, and A for positive
values of L and $\delta\ell$, particularly for great-circle arcs of Z = 76.33° or less. The
azimuths for other values of L or $\delta\ell$ are given in Table 1, adapted from GSFC [1974].

Note in Figure 3 that the curves become dashed for values of Z beyond 76.33°,
for which the elevation angle ε is less than 5°. For larger values of the great
circle arc and for lower elevation angles, the propagation-path parameters become
increasingly sensitive to atmospheric conditions [Bean and Thayer, 1959]. A common
system design criterion to avoid these effects is $\varepsilon \geq 5°$; hence, the curves of
Figure 3 are dashed-line curves when that criterion is not met. This will be
mentioned further in Section 3; see Appendix D.
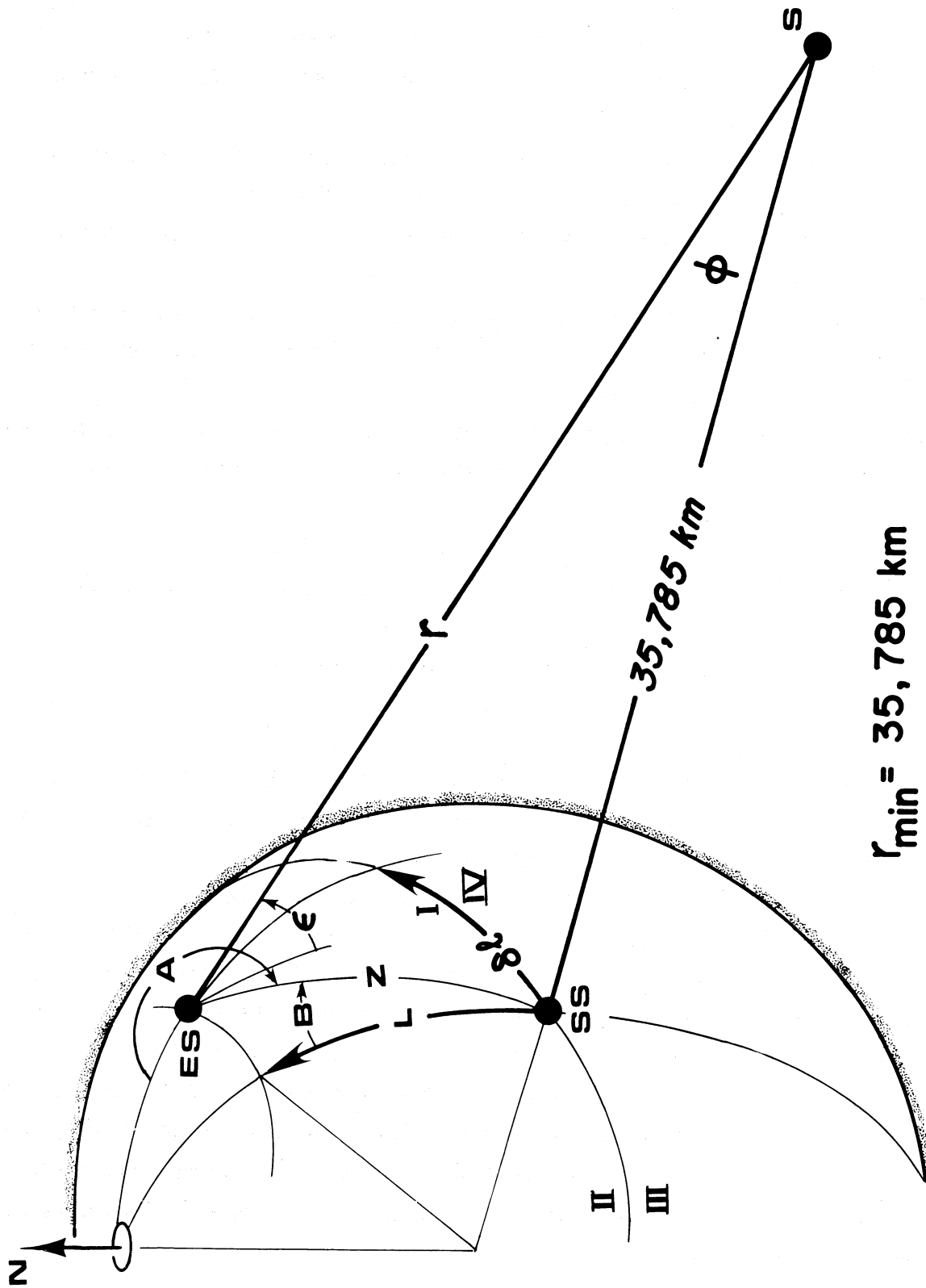
Figure 2. Identification of the ES/S path parameters and the ES/SS locational parameters for the synchronous satellite.

$r_{min} = 35,785 \text{ km}$
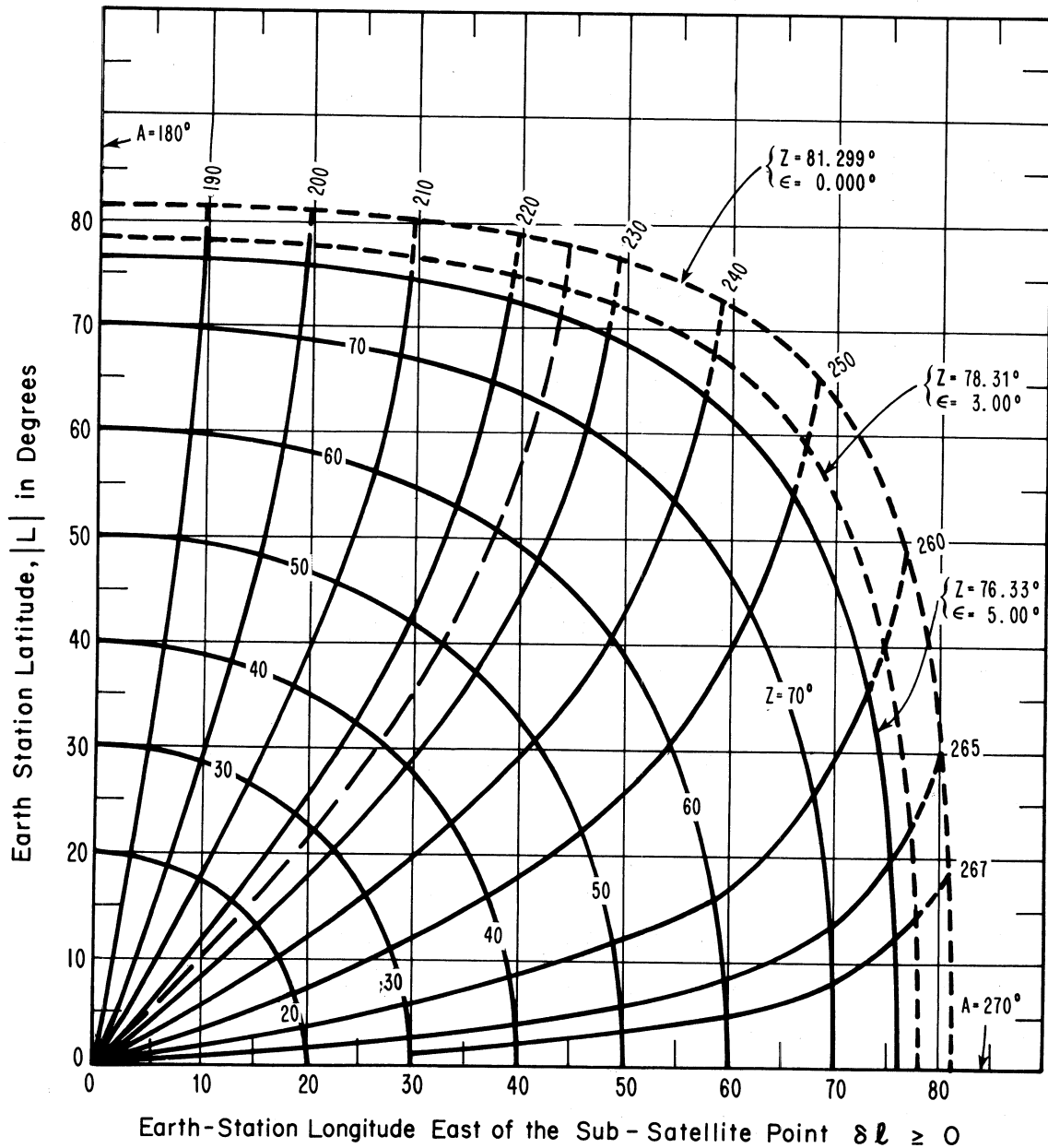
Figure 3. The great-circle arc (Z) and the azimuth (A) as a function of the
earth-station's north latitude (L) and for (δ𝑙) degrees of longitude
east of the sub-satellite point. The earth-station's elevation angle is ε.

7

Table 1. Tabulation of Azimuths, A, from ES to SS[†], as a Function of the ES Latitude L and the relative Longitude $\delta\ell$*

$\delta\ell < 0$		$\delta\ell > 0$	
$L \leq 0$	$L \geq 0$	$L \geq 0$	$L \leq 0$
A = 90°	A = 90°	A = 270°	A = 270°
80	100	260	280
70	110	250	290
60	120	240	300
50	130	230	310
40	140	220	320
30	150	210	330
20	160	200	340
10	170	190	350
0	180	180	360
QIII**	QII	QI	QIV

[†] Earth-station to sub-satellite point

* degree of longitude that ES lies <u>east</u> of SS

** <u>Q</u>uadrant number, see Figure 2

Figure A3 and Table A1 of Appendix A similarly relate L, $\delta\ell$, and Z with the back-azimuth B.

2.2 Disparate Definitions of Polarization

In the case of linear polarization, the definitions of horizontal and vertical is largely a matter of convention. For terrestrial systems, the definitions are given for each telecommunications link relative to a "plane of propagation" which contains both terminals and the great-circle path between them. Then:

the direction of <u>horizontal polarization</u> is defined as normal to the plane of propagation everywhere along the wave trajectory in that plane; and

the direction of <u>vertical polarization</u> is defined as lying in the
plane of propagation and everywhere normal to the radio wave
path trajectory in that plane.

These definitions are readily transferred to an antenna whose main beam is directed
along the radio wave path trajectory.

When these definitions are extended to the earth/synchronous satellite geometry,
we note:

a) The <u>horizontal polarization</u> directional vectors are <u>parallel</u>
for the two terminals of an earth-station/synchronous-satellite
(ES/S) link, but each is also lying in its respective local
tangential plane (at ES and at S).

b) The <u>vertical polarization</u> directional vectors for the two terminals
of an ES/S link are parallell, but do not normally coincide with
their local radial directions. They both lie in the plane defined
by the two terminals and the earth's center.

c) The definitions of vertical and horizontal polarization for
two or more ES/S systems will not coincide--even for the
same satellite--unless the ES are also co-located.

d) At a satellite, the vertical polarization directional vector
is always less than 8.7° above the satellite's horizontal plane
(see Figure 1). This horizontal plane is tangent to an imaginary
sphere through the satellite and concentric with the earth.

For transmissions between a satellite S_1 and its earth-station ES_1 (with great-circle
arc Z_1 and back-azimuth B_1, from SS_1 to ES_1), the linear polarizations (vertical and
horizontal) will appear to be rotated an angle θ_o from the orientations defined (for
vertical and horizontal) for another earth-station ES_2. See Appendix B for details.
If we designate the great-circle arc and back-azimuth from SS_1 to ES_2 as, respec-
tively, Z_2 and B_2, then we can also define

$$\delta Z = Z_1 - Z_2 \qquad \text{and} \qquad \delta B = B_1 - B_2. \qquad\qquad (3a,b)$$

Figure 4 is a plot of θ_o, the apparent angle of rotation, for any linearly polarized
transmissions directed from S_1 to ES_1 but as received by ES_2. This apparent angle
of rotation, due entirely to the geometrical disparity of definitions, is plotted
relative to δB, the disparity in back-azimuths. Although θ_o is also a function of
δZ, the dependency is so slight that, to a good approximation (within a degree)

$$\theta_o \simeq \delta B \qquad\qquad (3c)$$

and

$$XPD \simeq -20 \log |\sin \delta B|. \qquad\qquad (3d)$$

Since this linear depolarization angle can vary appreciably, Figure 4 suggests that linear polarization is not suitable for large earth-area coverage, but is quite useful for co-channel isolation over small coverage areas ($\delta B < 5°$ or $10°$). Appendix C details the expressions for circular polarization so that it can be seen that the effect of the depolarization of Figure 4 is negligible for circular polarization. The generation of opposite-sense circular polarization would be associated only with unequal rotation or attenuation of orthogonal linear polarizations. The effect of δB is to merely provide additional rotation of the circular polarization.

2.3 Numerical Example for the Effects of Geometry

Consider a synchronous satellite S_1, with a subsatellite point SS_1 (on the equator) at say 114° W longitude (west of Greenwich, England). For an earth station ES_1 at approximately 38° N latitude and 77.5° W longitude (near Washington, D. C.), the ES_1 lies $\delta\ell = 36.5°$ east of the SS_1 point. From Figures 1, 3, and A3

for $\qquad\qquad L = 38° \qquad\qquad \delta\ell = 36.5°$

we read off $\quad Z_1 \simeq 52° \qquad\qquad \varepsilon_1 \simeq 30°$

$\qquad\qquad r_1/R_0 \simeq 6.047° \qquad \phi_1 \simeq 7.4°$

$\qquad\qquad A_1 \simeq 229° \qquad\qquad B_1 \simeq 36°$

and then determine the range as

$$r_1 = (6.047)\ 6378 = 38{,}568 \text{ km.}$$

For an earth station at Anchorage ($L \simeq 61°N$, $\delta\ell \simeq 36°$), Figures 1, 3, and A3 yield

$\qquad Z_2 = 67° \qquad\quad \varepsilon_2 = 14.3° \qquad\qquad \phi_2 = 8.4°$

$\qquad A_2 = 220° \qquad\quad B_2 = 18° \qquad\qquad r_2/R_0 = 6.285$

so that $r_2 = (6.285)6378 = 40{,}086$ km.
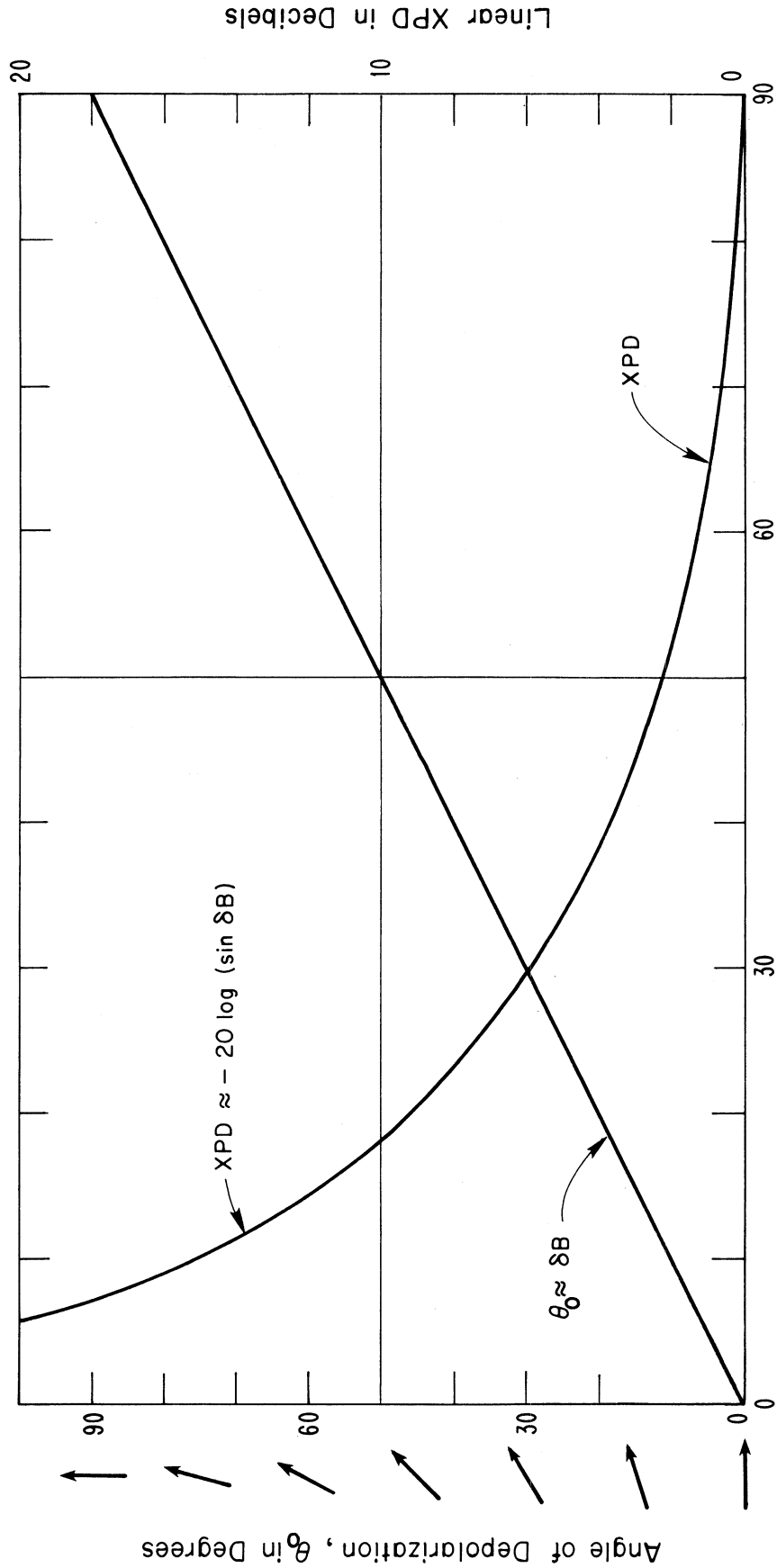
Figure 4. Apparent rotation of the linear polarization vector (angle of depolarization, θ_0) and cross-polarization discrimination (XPD in decibels). These result solely because of geometry and the disparate definitions of polarizations for earth stations differing in their back-azimuths B from a sub-satellite point.

If the transmissions from S_1 to ES_1 are monitored at ES_2, a linearly polarized signal will appear to have suffered a depolarization given by an angle of rotation of $\theta_o \approx 18°$, as determined from Figure 4 or (3b) and (3c) for $B_1 = 36°$,

$$\theta_o \approx \delta B = B_1 - B_2 = 36° - 18° = 18°.$$

That is, a vertically polarized transmitted signal will appear to be oriented 18° clockwise from vertical (or 108° clockwise from horizontal) and an originally horizontally polarized signal will appear to have a polarization oriented at 18° from the horizontal.

For an ES_1/S_1 downlink at say f = 12.6 GHz, the free-space basic transmission loss--from the first three terms of (2) is*

$$\begin{aligned} L_{bo} &= 92.45 + 20 \log (12.6) + 20 \log (38,568) \\ &= 92.45 + 22.01 + 91.72 = 206.18 \text{ dB}. \end{aligned}$$

From Figure 1, we note that the range of r/R_0 varies approximately between 5.61 and 6.53. Converted to range (by the factor $R_0 = 6378$ km), then

$$20 \log r = 91.73 \pm 0.66 \text{ dB}.$$

For
$$\varepsilon \geq 5°, \ r \leq (6.441) \ 6378 = 41,081,$$
and
$$L_{bo} \leq 92.45 + 20 \log (41,081) + 20 \log f \approx 185 + 20 \log f$$

or less.

To determine the free-space loss of (1) and (2) for this S_1 system, we note first that the polarization discrepancy $\theta_o = 0$ would provide a mis-matched linear polarization loss for reception at ES_1 of

$$\delta_o = \cos \theta_o = 1.0 \qquad \text{and} \qquad -20 \log \delta_o = 0 \text{ dB},$$

---

* Note that logarithm "to the base 10" will be understood from here on, so that we may omit the subscript 10 from the $\log_{10}$. Further, the number of significant digits employed is to facilitate the reader's following of the numerical example and does not imply an accuracy of estimates for the initial parameter values.

but for reception at ES_2

$$\delta_o = \cos 18° = 0.951, \qquad \text{and} \qquad -20 \log \delta_o = 0.44 \text{ dB}.$$

Also required is a knowledge of the system antenna gains. For reference, the power gains (as a power ratio g or as G in dBi) are given in Table 2 for several elementary or common configurations [EEH, 1975]. A useful additional expression is that relating the half-power beamwidth in degrees to the antenna power gain [Skolnik, 1970, p. 9-5].

$$\Omega^2 = (360)^2/\pi g´ \qquad , \qquad g´ > 3. \tag{4}$$

Here Ω^2 is either the square of the beamwidth of an axially symmetrical antenna configuration or the product of the beamwidths in the E and H planes. For the frequency f in gigahertz, the dish diameter D in meters and $\eta = 0.55$, expression (4) may be combined with that for the dish in Table 2 to obtain

$$\Omega \approx 26.2/(fD) \approx 19.4/(fD\sqrt{\eta}) \ . \tag{5}$$

Table 2[†]. Power Gains for Some Common Antennas*

Antenna Type	gain above isotropic g´	in decibels G´
Isotropic	1.0	0.00
Elementary Dipole	1.5	1.76
Half-wave Dipole	1.64	2.15
Optimum Horn	$10 \ S/\lambda^2$	$20.46 + 20 \log f + 10 \log S$
Broadside Array	$4 \ S/\lambda^2$	$16.48 + 20 \log f + 10 \log S$
Parabolic Dish	$\eta(\pi D/\lambda)^2$	$20.4 \ + 20 \log f + 20 \log D + 10 \log \eta$
or	$4\pi\eta S/\lambda^2$	$21.45 + 20 \log f + 10 \log S + 10 \log \eta$
		$9.94 + 20 \log (D/\lambda) + 10 \log \eta$

[†] S is the aperture area in square meters, D is the dish diameter in meters, λ is the radio wavelength in meters, f is the radio frequency in gigahertz, and η is the antenna efficiency (≈ 0.5 to 0.65).

* Exclusive of line and radome losses, as indicated by the primes on g and G.

Consider the ES_1/S_1 system; let us assume that a spot coverage area required a half-power beamwidth restricted to within a radius of 445 km about the earth station. That restriction reduces to 445/111.32 or 4.0° of arc. From the information determined at the start of this subsection, $Z_1 = 52°$, so that we must consider $48° < Z < 56°$. From Figure 1, this corresponds to $7.15° < \phi < 7.85°$ or a vertical-plane beamwidth of $7.85° - 7.15° = 0.7°$ and a horizontal-plane beamwidth of $890/38,568 = 0.02308 = 0.023$ radians or 1.35°. For a dish, the 0.7° would govern; from (5) for $\eta = 0.55$, a dish of

$$D \approx 26.2/(12.6)(0.7) \approx 3 \text{ m}$$

diameter would be required.

Of course, the service area determined on the earth's surface by a symmetrical antenna configuration is usually neither circular nor necessarily well defined. It is oval, perhaps truncated by the horizon ($\varepsilon = 0$), with the area for which $0° \leq \varepsilon < 5°$ determined by the variable localized refractivity structure (see Appendix D). For an earth-station dish antenna of diameter $D_{ES} = 10$ m, from Table 2,

$$G'_{ES} = 20.4 + 20 \log (12.6) + 20 \log (10) + 10 \log (0.55)$$
$$= 20.4 + 22.01 + 20 - 2.6 = 59.81 \text{ dBi}.$$

Assuming $D_S = 3$ m for the satellite dish antenna, then from Table 2

$$G'_S = 20.4 + 22.01 + 20 \log 3 + 10 \log (0.55)$$
$$= 42.41 + 9.54 - 2.6 = 49.35 \text{ dBi}.$$

We assume line and radome losses of $L = 1.0$ dB. Since $G = G' - L$, $G_{ES} = 58.81$ dBi, $G_S = 48.35$ dBi. For the ES_1/S_1 link then, the free-space transmission loss is given by (2) as

$$L_o = 92.45 + 20 \log (12.6) + 20 \log (38,568)$$
$$- 48.35 - 58.81 - 20 \log (\cos 0°)$$
$$L_o = 206.18 - 107.16 + 0.0 = 99.02 \text{ dB}.$$

For a similar ES_2/S_1 link, for which $r = 40,086$ km and $\theta_o = 18°$

$$L_o = 95.36 - 20 \log (\cos 18°) = 99.8 \text{ dB}.$$

14

3. ENVIRONMENTAL EFFECTS

The environment in which earth/satellite systems operate has profound effects upon those systems. The satellite orbit described in Section 2 and Appendix A is determined by the earth's gravitational field. The external noise background for the earth/satellite system is the contribution of the earth and other celestial bodies. In addition, we are concerned with the other effects of the earth's atmosphere in which the earth station is immersed. The "earth station" is not necessarily fixed on the earth's surface, it might be mobile, on the surface, or airborne aloft; it could consist of a multiplicity of locations within a broadcast satellite's service area. In each case, it is immersed within the lower troposphere, within about 15 km of the surface; the system signal must traverse the remainder of the troposphere, stratosphere, and ionosphere subject to their influences.

3.1 Atmospheric Effects

There are several phenomena, such as the refraction, absorption, and scattering of radio waves by the gaseous atmosphere and hydrometeors (fog, clouds, rain, hail, snow, etc.) which refract, attenuate, delay, and depolarize earth/satellite signals. Their effects include [CCIR, 1978a; Bean et al., 1960]:

    (a)   loss of signal due to beam-divergence of the earth-station antenna because of atmospheric refraction;

    (b)   decrease in effective antenna gain due to phase decorrelation across the earth-station antenna aperture, caused by irregularities in the refractive-index structure;

    (c)   possible limitations in bandwidth due to multiple scattering or multipath effects;

    (d)   attenuation by the local environment of the earth terminal (by buildings, trees, etc.);

    (e)   relatively slow fading due to beam-bending caused by large-scale changes in refractive index and somewhat more rapid fading (scintillation) and variations in the earth-station angle (of arrival or launch), due to small-scale variations in the tropospheric or ionospheric refractive index;

    (f)   emission noise from atmospheric absorption;

    (g)   signal attenuation due to absorption and scattering by: the gaseous atmosphere, the water droplets and ice crystals in clouds, and precipitation; and

(h) signal depolarization by the water droplets and ice crystals of precipitation and clouds.

Each of these effects is described by observational data summarized in recent CCIR Reports [CCIR, 1978a and 1978b]. However, the effects of items (a) through (d) above are avoidable and will become negligible for proper site selection and for the design requirement which specifies that the earth-station elevation angle be constrained to $\varepsilon \geq 5°$. Even this last constraint may be removed by the use of adaptive transmission and reception techniques which would compensate for the atmospheric variability [Crane, 1976,1978].

As an indication of what can be expected for item (e) above, observations of beam-bending at about 16 GHz are shown in Figure 5 adapted from Bean and Dutton [1968]. There, the median total refraction angle, $\overline{\varepsilon - \varepsilon_o}$ in milliradians, and its standard deviation, $S(\varepsilon - \varepsilon_o)$ in milliradians as a measure of tropospheric scintillation, are plotted versus the geometrical angle ε_o. For the standard deviations, $S'(\varepsilon - \varepsilon_o)$ including the total of both tropospheric and ionospheric scintillations [CCIR, 1978b], over the range of $0.3 \leq f \leq 30$ GHz, use

$$S'(\varepsilon - \varepsilon_o) \approx S(\varepsilon - \varepsilon_o) [1 + (0.3/f)^2]^{1/2} \tag{6}$$

The items (f), (g), and (h) above are described in the subsections below.

3.1.1 Noise

The system equivalent noise density at a receiving terminal is separable into that arising external to the receiving system and that generated within the receiver. The noise levels associated with external sources are generally expressed in terms of equivalent temperatures, T_e in degrees Kelvin or in decibels above a reference temperature (290°K). The external noise-power spectral density is given by

$$n_e = k T_e \quad \text{watts/Hz} \tag{7}$$

where k is the Boltzman constant, $1.38(10)^{-23}$ watts/(Hz°K). Therefore

$$N_e = 10 \log n_e = -228.6 + 10 \log T_e \quad \text{dBW/Hz} . \tag{8}$$

The external noise temperature must be added to the receiving system's equivalent noise temperature, T_R in °K, to determine the total system noise,
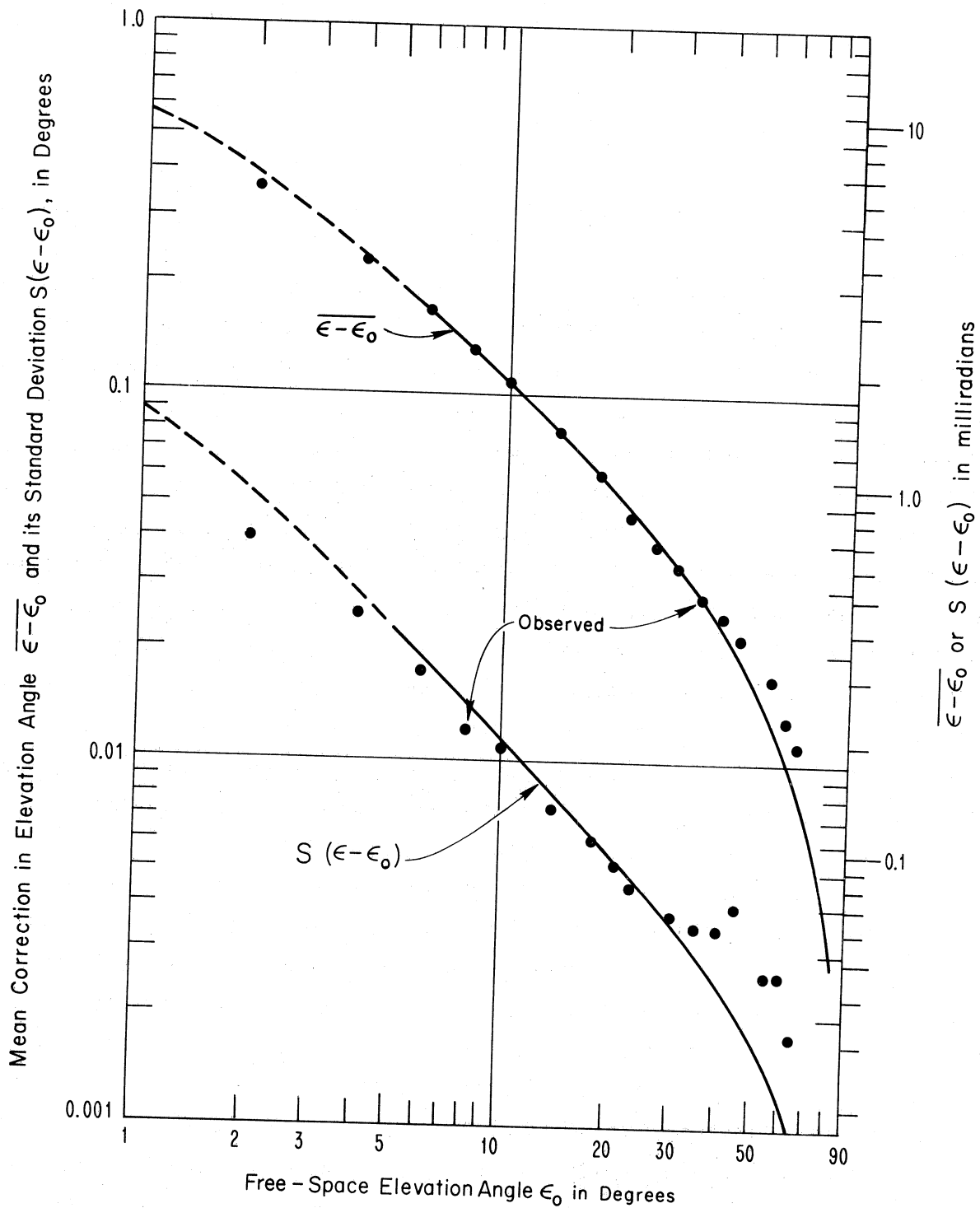
Figure 5. Observed and predicted effects of tropospheric refraction and scintillation upon an earth-station's elevation angle ε [adapted from Bean and Dutton, 1968].

17

$$n = k(T_e + T_R) \; Bw \; \text{watts} \tag{9}$$

or

$$n = k(T_e + f_R \; 290°K) \; Bw \; \text{watts}, \tag{10}$$

where Bw is the system noise bandwidth in hertz. The receiver equivalent noise temperature and the reference 290°K are related by the receiving system noise figure f_R.

For an ES/S downlink, the earth-station's receiver sees the noise sources associated with the earth's atmosphere, possibly the sun and moon, and the galaxy beyond. The equivalent noise temperatures associated with these external sources are shown in Figure 6 as a function of radio frequency [CCIR, 1978c, 1978d]. The sun (which subtends an angle of about 0.5° from the earth) constitutes the strongest source of noise unless the receiving antenna and its initial sidelobes are directed away from it. Ordinarily, galactic noise (curve G in Figure 6) tends to be dominant over most of the UHF range, but in some locations, business-area man-made noise (such as curve M in Figure 6, for example) may dominate. A lower bound on external noise is provided by background cosmic noise (curve B for black-body radiation) over the upper UHF/lower SHF and usually by the gaseous atmosphere (curve CS for clear sky) at the upper SHF and higher frequencies for selected values of the ϵ elevation angle. However, at SHF, very often clouds and occasionally rainfall contribute to atmospheric noise as sources that occur only for small percentages (p in %) of a year. See (17a) in Section 3.3.

For an ES/S uplink, the satellite receiver looks toward the earth. For spot beam coverage, seeing portions of the earth's surface, the equivalent noise temperature (now called apparent temperature) may be that observed over the open sea or land with either vegetative or (perhaps) a snow cover. Some apparent temperatures, observed at specific frequencies, are listed in Table 3. If moderate to heavy rainfall occurs over the spot-beam coverage area, the rainfall will provide increased temperatures for frequencies of 6 to 8 GHz and above. For a general earth-coverage satellite antenna, the resulting land/sea integrated value will approximate that for the sea surface values of Table 3. Then, when rainfall occurs, it is not likely to be sufficiently widespread to further increase the integrated apparent temperature [CCIR, 1978c].
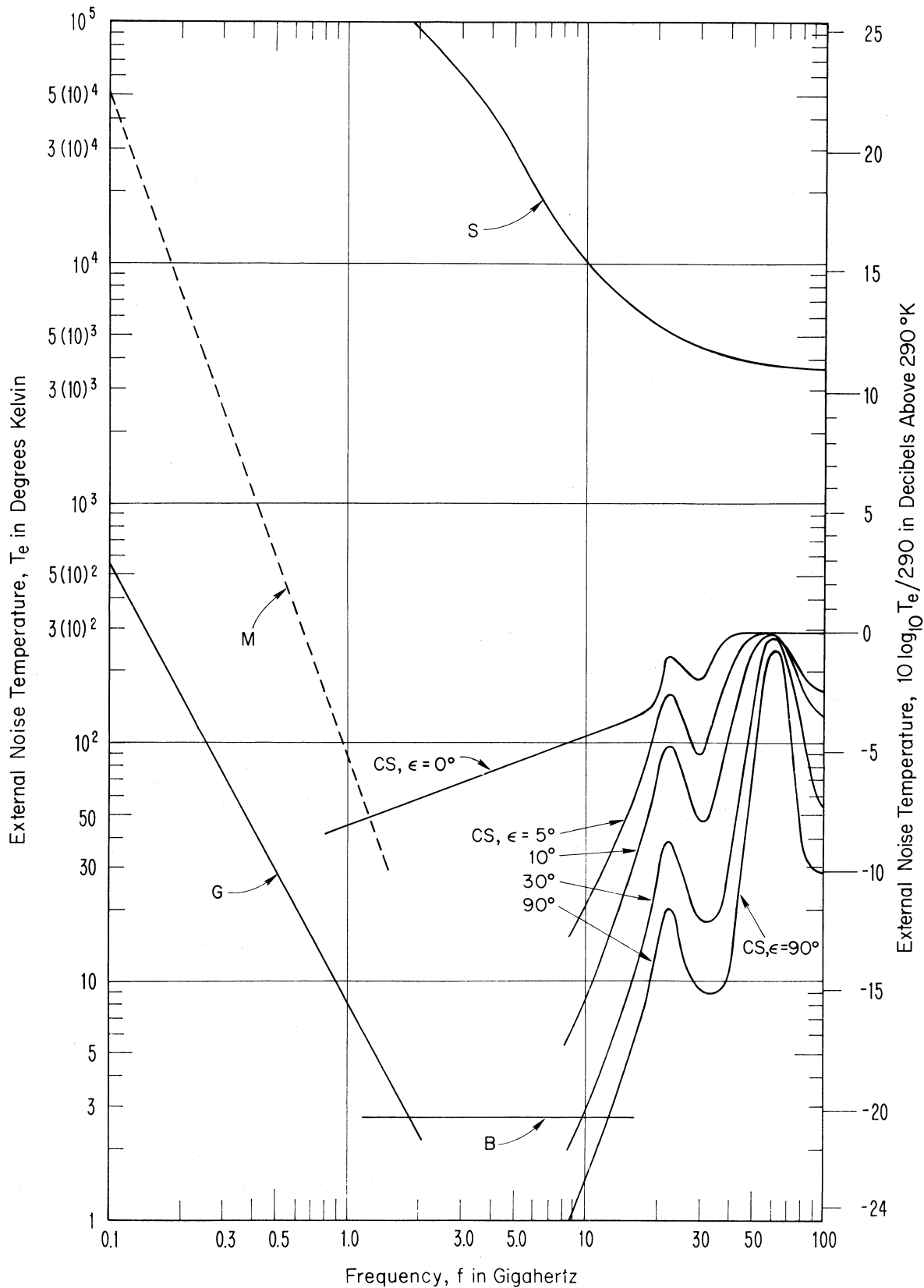
Figure 6. Apparent temperatures of various external noise sources for downlink slant paths. The noise sources are identified by M for man-made, G for Galactic, B for black-body, S for solar, and CS for clear-skies, and the indicated values of the elevation angle ε.

Table 3.[†]   Apparent Temperatures, T in °K, of External Noise Sources
             on Uplink Slant-paths

NOISE SOURCE	OBSERVATIONAL FREQUENCY, GHz						
	1.4	3	5	10	10.6	13.6	37.5
Sea Surface*	93 to 94			105 to 115			168 to 178
Vegetated Land[††]	235 to 270	255 to 275			282		
Snow**			265 to 275			205 to 263	195 to 265

[†] CCIR inputs indicate that the Interim Meetings of Study Group 5 is planning
     to produce a curve of uplink external noise temperatures versus frequency

[††] Varies with moisture content of soil

 *   Varies with water temperature, salinity, surface wind speed

 ** Varies with equivalent water content

3.1.2   Atmospheric Attenuation

The atmospheric limitations on slant-path (ES/S) systems are not confined to
its contributions to system noise. In addition, the atmosphere attenuates (by
absorption, scattering, and depolarization) the radio signals that traverse it. For
example, the gaseous atmosphere, by virtue of its constituents (water vapor, oxygen,
pollutants, etc.) and their state (temperature, partial pressure, etc.) attenuates
a signal by an amount $A(f,H,\varepsilon)$ in decibels, that varies with the radio frequency f,
the initial height H above mean-sea-level (MSL) of the earth-station, and the ele-
vation angle ε at that earth-station. For the longer propagation paths through the
atmosphere at lower elevation angles,

$$A(f,H,\varepsilon) = A(f,H,\varepsilon = 90°)/\sin \varepsilon, \qquad 5° \leq \varepsilon \leq 90° \tag{11}$$

where $A(f,H,\varepsilon = 90°)$ are the values for a vertical path [CCIR, 1978e].

In Figure 7, the attenuation values are plotted for the conditions $\epsilon = 30°$, $H = 0$. There it has been relabeled as $A(p = 50\%)$, the attenuation by the ubiquitous gaseous atmosphere at a locale near Washington, D. C. The curve $A(p = 10\%)$ shows the added effect of non-precipitating clouds. The curves $A(p)$ for $p \leq 2\%$ show the additional attenuation associated with precipitating clouds and rainfall. There is an atmospheric attenuation peak in the clear-air at $f \simeq 22$ GHz and a corresponding "window" or attenuation minimum near 30 GHz. From Figure 7, it is clear that this window is available for all but about 20% of the year; then it becomes increasingly "opaque" because of attenuation by clouds and rainfall.

For the attenuation by the gaseous atmosphere, the non-precipitating clouds and for the lighter rainfall, the inverse-sine-law (the cosecant law) of (11) is applicable. Regardless of the f and H values, we can write

$$A(p,\epsilon) = A(p, \epsilon = 30°)/2 \sin \epsilon \qquad (12)$$

for $5° \leq \epsilon \leq 90°$; $1\% \leq p < 100\%$.

The factor 2 in the denominator of (12) is to convert the attenuation value from Figure 7 where $\epsilon = 30°$ to that for $\epsilon = 90°$. The factor $\sin \epsilon$ in the denominator converts the zenith value ($\epsilon = 90°$) to that for an arbitrary elevation angle. This simple adjustment factor for ϵ is not applicable for the attenuations associated with higher rainfall rates (>5 mm/hr). Some such simplified correction factors have been proposed for rainfall rates of 5 mm/hr and more, but these are still under investigation [CCIR, 1978a; ITU, 1979].

3.1.3   Signal Depolarization

The Section 2.2 and Appendices A and B described the effective depolarization or angular rotation, θ_o, of the linear polarization vector (observed as a geometrical or free-space rotation on ES/S slant paths) directly attributable to the definitions of linear polarization. In addition to this, there is a further rotation of the signal's polarization vector imposed by the atmosphere. In traversing the ionosphere, the signal experiences a Faraday rotation, approximated by [CCIR, 1978b]

$$\theta_i = 108°/f^2 \qquad (13)$$

for the frequency f in gigahertz. The disparate polarization loss is now given by 20 log δ, where
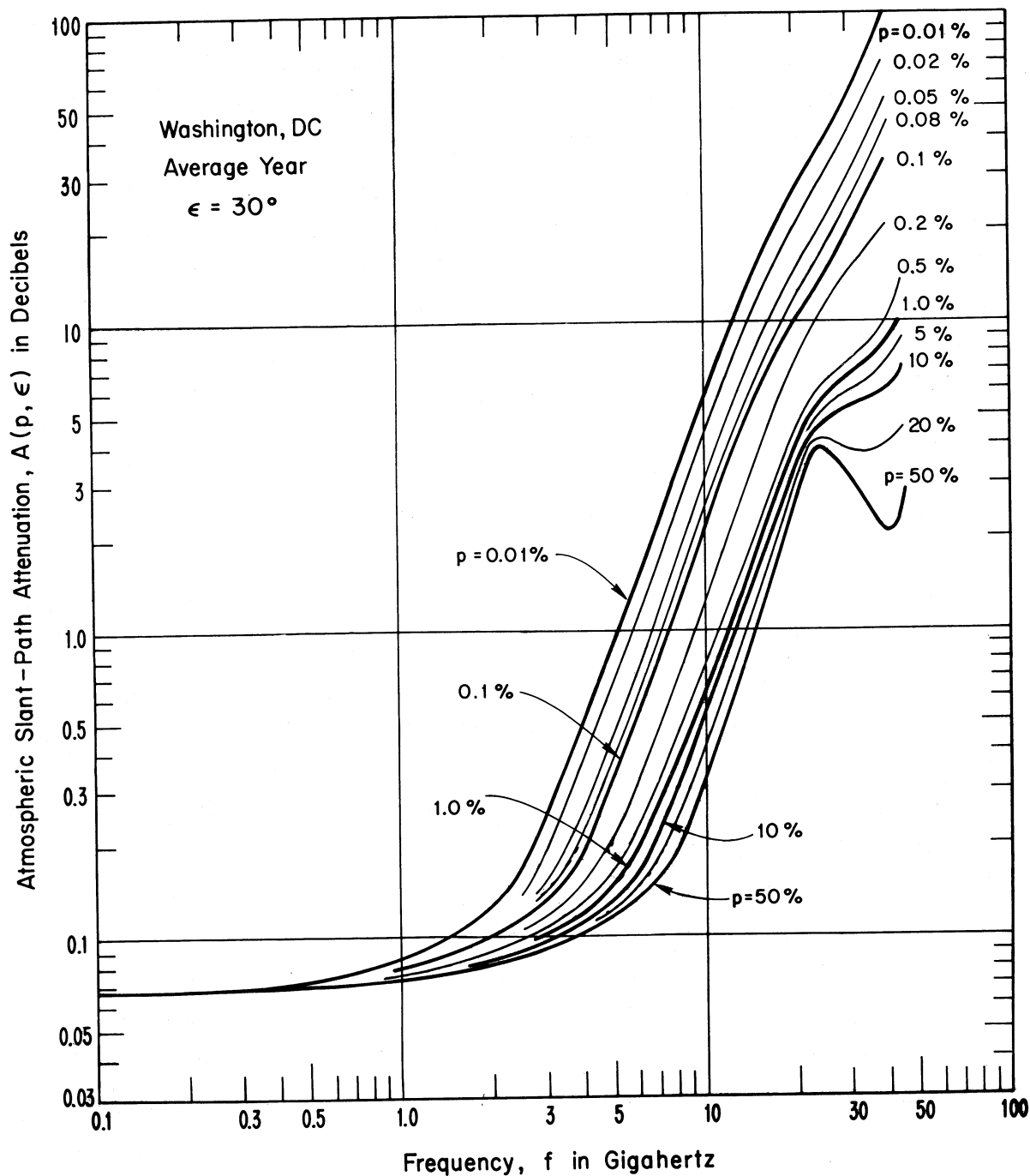
Figure 7. Predicted atmospheric attenuation versus frequency for an
earth-station near Washington, D. C., and an elevation angle
of ε = 30°. Clear-sky conditions correspond to p = 50%. That
and the additional effects of non-precipitating clouds is for
5% < p < 20%. The effects of including increasingly heavy
rainfalls is indicated by 0.01% < p < 1%.

$$\delta = \cos(\theta_o + \theta_i) \tag{14a}$$

$$= \cos(\delta B + 108/f^2) . \tag{14b}$$

There is a further depolarization in traversing rainfall and clouds in the troposphere. Estimates of the attenuation by clouds and rainfall described in the previous subsection include this co-polarized signal attenuation; i.e., CPA = $A(p,\varepsilon)$.

We will return to this depolarization effect again in the section under interference fields.

3.2 Service Fields

Of course, the interest in atmospheric effects is for the determination of service fields, the determination of the system parameters (transmitter power, antenna gains, etc.) that would be required to achieve the desired service field. Paralleling (1) and (2), we can express the received signal from

$$P_R = P_T - L_{bo} + G_T + G_R + 20 \log \delta - A(p,\varepsilon) \quad \text{dBW} \tag{15a}$$

$$= P_T - L = P_T - L_o - A(p,\varepsilon) \quad \text{dBW} \tag{15b}$$

where

$$L = L_o + A(p,\varepsilon) = L_o + \text{CPA} \quad \text{dB} \tag{15c}$$

$$= L_{bo} - G_T - G_R - 20 \log \delta + A(p,\varepsilon) \quad \text{dB} \tag{15d}$$

The quantities are all defined as for equations (1) and (2), except that:

δ is the loss factor due to the polarization discrepancy (geometrical and ionospheric rotation of the transmitted signal's polarization vector) given by (14b);

$A(p,\varepsilon)$ is the co-polarized signal attenuation, CPA, due to the atmosphere, for p% of an average year and an earth station elevation angle ε.

3.2.1   The Co-polarized Attenuation

There are a variety of procedures for determining the co-polarized attenuation, $A(p,\varepsilon)$ all in varying degrees of development and growth [CCIR, 1978a, 1978e, 1978f, 1978g, 1978h; GSFC, 1978]. One procedure is available as a computer program DECP77 to determine the annual distribution of the attenuation of microwaves by rainfall for earth-stations at the surface [Dutton, 1977; Dutton and Dougherty, 1978]. The program is available from E. J. Dutton at the Boulder Laboratory facilities of NTIA/ITS [(303) 497-3646 or FTS 320-3646]. Alternatively, one can determine for a

given location in the USA, the surface rainfall rate applicable for p percent of (for example) 99 out of 100 years [Dutton and Dougherty, 1979]. Then, one determines the attenuation coefficient in dB/km and the effective slant-path length; their product is the total attenuation [Crane, 1980].

Figure 8 is the distribution (in percent of all hours of the year) of the total attenuation $A(p,\varepsilon)$ determined by DEGP77 for signal transmissions at 12.6 GHz from or to a fixed earth-station in the vicinity of Washington, D. C., for an elevation angle $\varepsilon = 30°$ [Dutton, 1977]. The central, dashed-line curve is the reference distribution for an average year. This plot coincides with values from the curves of Figure 7 for f = 12.6 GHz. The most striking feature of rainfall and of attenuation by rainfall is, of course, its variation both from one-locale-to-another and from one-year-to-the-next [Dougherty and Dutton, 1978; Dutton and Dougherty, 1979]. This variation is depicted by the solid-line curves of Figure 8, within which an observed annual distribution of attenuation would be expected to fall for nine out of ten years. Similarly, the dash-dot curves mark the bounds for observed distributions of 99 out of 100 years. The attenuation for $p \geq 50\%$ is attributable to the gaseous atmosphere, that for $p > 20\%$, is attributable to the effects of non-precipitating clouds and the gaseous atmosphere. For rainfall rates of 3, 14, and 70 mm/hr ($p \leq 1.0\%$, 0.1%, and 0.01% near Washington, D. C.), the attenuation is increased for increasingly heavy rainfall. Again, for $p \geq 1\%$, the atmospheric attenuation follows the cosecant law of (11), i.e.,

$$A(p,\varepsilon) = A(p,\varepsilon = 30°) \cdot (0.5/\sin \varepsilon), \tag{16}$$

for $1\% \leq p \leq 100\%$ and $5° \leq \varepsilon \leq 90°$.

3.2.2   Site Diversity

In Europe and North America, the strong attenuation is associated with the heavier, intense, convective rainstorms that are often of limited horizontal extent (of the order of a few kilometers). Much of this extreme attenuation might therefore be avoided by site diversity, the use of two or more spaced terrestrial terminals. If their horizontal spacing is sufficient, the likelihood of reception (at one of the terminals) without serious attenuation by rainfall can be increased to the desired design probability level.

Report 564-1 [CCIR, 1978a] summarizes the available site diversity data and makes some tentative recommendations. From experimental data, a relationship has been derived between the cumulative probability of attenuation for a single site, p_1, and the joint probability for a pair of sites, p_2, for (diversity) site

24
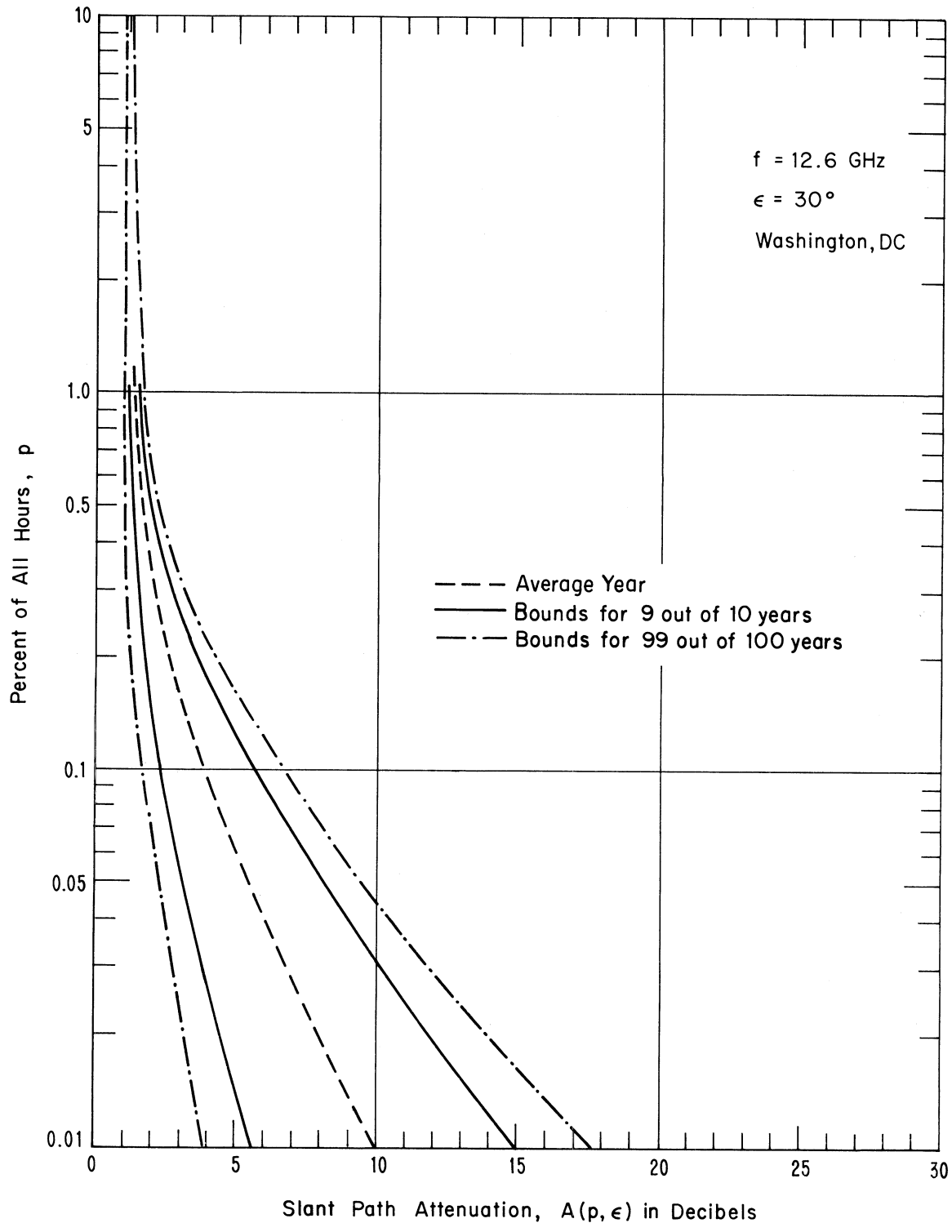
Figure 8. Predicted distributions of the total slant-path atmospheric
attenuation at 12.6 GHz and $\epsilon = 30°$ as a percent (p) of all
hours of a year.

separations of 2 to 50 km. This is presented in Figure 9, adapted from CCIR [1978a]. There, the plotted curves are identified by the value of single-site cumulative probability of attenuation by rainfall. For the same attenuations, the curves of Figure 9 relate the necessary site diversity spacing to reduce the probability to the desired joint cumulative probability. The ratio of the single-site probability to the joint probability , p_1/p_2 (for the common attenuation), is known as the diversity advantage factor. The difference in attenuation

$$\delta A(p) = A(p_2) - A(p_1) \tag{17}$$

is a measure of the additional signal margin provided by the site diversity. Generally, a fairly detailed relationship between the site diversity spacing and the diversity advantage, p_1/p_2 or $\delta A(p)$, is required in order to assess either the return on the sizable economic investment versus the reduction in telecommunication outage probability or alternative ways of achieving the margin $\delta A(p)$. The sizable investment arises either from the necessary duplication of terrestrial terminal facilities and their associated terrestrial-links to a central processing point or from an increase in transmitter power, antenna gains, etc.

3.3 Numerical Example for Environmental Effects

Consider the earth-station/synchronous satellite system ES_1/S_1 whose downlink geometry was described in subsection 2.3. Recapitulating in the notation following (1) and (2) in subsection 1.1 and in subsection 2.1, the earth-station ES_1 is fixed and near Washington, D. C. (38°N latitude and 77.5° W longitude); the subsatellite point SS_1 on the equator is at 114° W longitude.

$$\delta \ell = 36.5°, \qquad Z_1 = 52°, \qquad \varepsilon_1 = 30°,$$
$$A = 229°, \qquad B_1 = 36°, \qquad \phi_1 = 7.4°,$$
$$r_1 = 38,568 \text{ km}.$$

Also

$$f = 12.6 \text{ GHz} \qquad D_S = 3 \text{ m}, \qquad G_S' = 49.35 \text{ dBi}, \qquad G_S = 48.35 \text{ dBi}$$
$$\theta_0 = 0° \qquad D_{ES} = 10 \text{ m}, \qquad G_{ES}' = 59.81 \text{ dBi}, \qquad G_{ES} = 58.81 \text{ dBi}$$
$$L_0 = 99.02 \text{ dB}.$$

In order that a specified downlink transmitter power, P_T, achieve a desired grade of service, it is required that the received signal carrier-to-noise ratio in decibels be more than (c/n) dB for 100 - p (or for all but p) percent of the hours

26
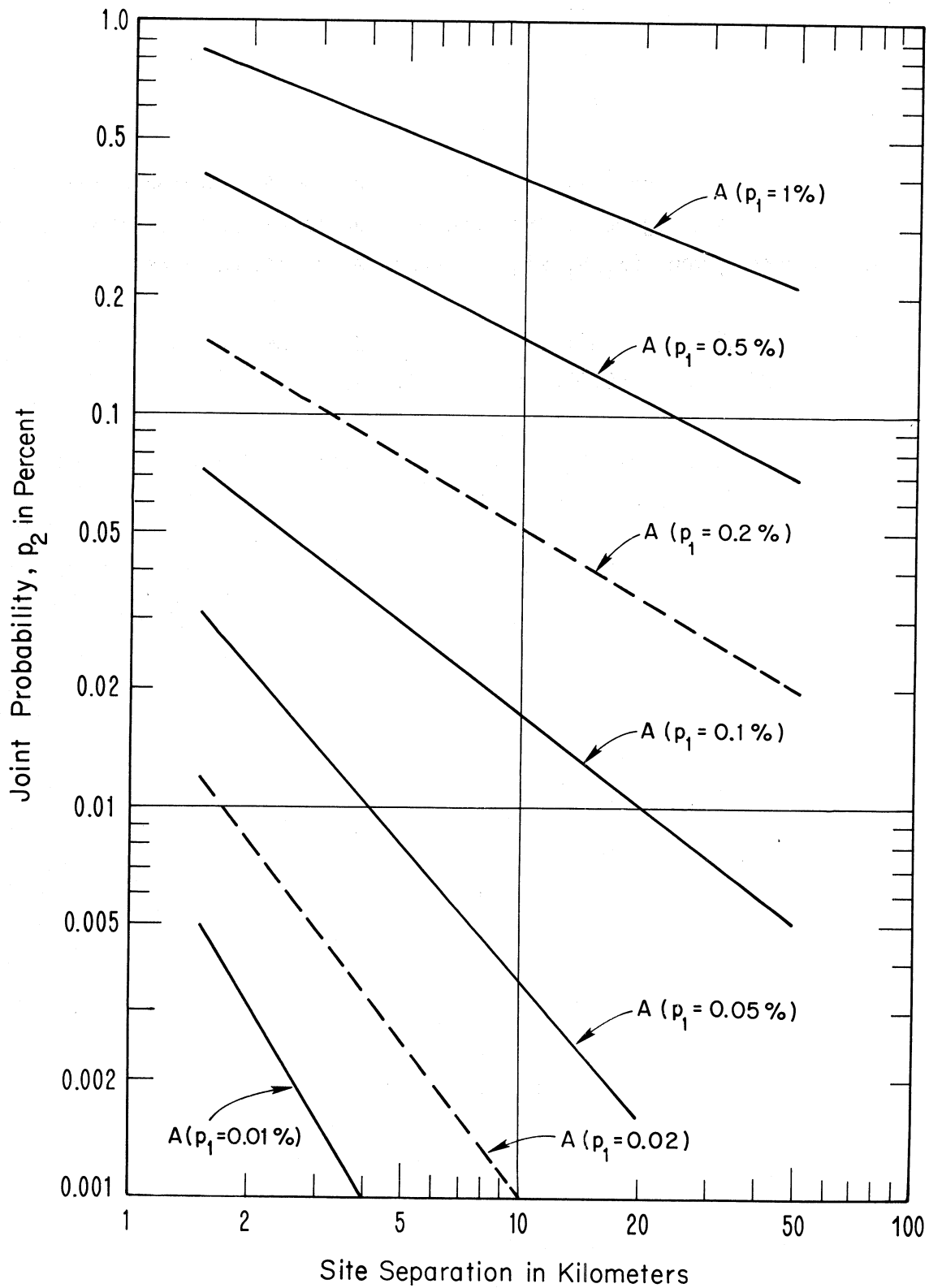
Figure 9. The joint probability, p_2, in percent of all hours of the year that the atmospheric attenuation will not exceed $A(p_1)$ at one or the other of two separated sites (earth-stations). $A(p_1)$ is the attenuation exceeded at either site for p_1 percent of all hours of the year ($p_2 < p_1$).

of a year. Therefore, we require that

$P_T = 0$ dBW   (c/n) dB = 15 for p = 0.01%
$f_R = 1.5$ Bw = $4(10)^7$ Hz.

We specify that the sun and moon will not fall within the ES_1 antenna main beam and major side lobes; then from Figure 6, the greatest source of noise at f = 12.6 GHz is the rainy atmosphere. When ES_1/S_1 signals experience attenuations

A(50%,30°) = 1.1 dB,   A(1%,30°) = 1.25 dB,   A(0.45%,30%) = 1.7 dB,
A(0.1%,30°) = 6.82 dB,   A(0.01%,30°) = 17.7 dB,

(from Figure 9 for the upper bound of 99 out of 100 years), their equivalent noise temperatures are approximated by [GSFC, 1978]

$$T_e(p,\varepsilon) = 290 \left[1 - 10^{-0.1A(p,\varepsilon)} \right] \tag{17a}$$
and
$$T(p,\varepsilon) = T_e(p,\varepsilon) + f_R\, 290 \tag{17b}$$

as

$$T(0.01\%,30°) = 290 \left[1 - 10^{-1.77} \right] + 1.5(290)$$
$$= 290\, [1 - 0.01698] + 435$$
$$= 290\, [0.9830] + 435$$
$$= 285 + 435 \quad = 720°K$$

T(0.1%,30°) = 229.7 + 435   = 664.7°K
T(0.45%,30°) = 93.9 + 435   = 528.9°K
T(50%,30°)   = 64.9 + 435   = 499.9°K .

From (8), (9), and (10), the total noise power is

$$N(p) = -228.6 + 10 \log Bw + 10 \log T$$
$$= -228.6 + 10 \log (4.10^7) + 10 \log T \tag{17c}$$
$$\equiv -152.6 + 10 \log T \text{ dBW}$$

For the total temperatures determined above,

$$N(0.01\%) = -152.6 + 10 \log (720) \quad = -124 \text{ dBW}$$
$$N(0.1\%) \ = -152.6 + 10 \log (664.7) = -124.37 \text{ dBW}$$
$$N(0.45\%) = -152.6 + 10 \log (528.9) = -125.37 \text{ dBW}$$
$$N(50\%) \quad = -152.6 + 10 \log (499.9) = -125.61 \text{ dBW}$$

From (13), note that

$$\theta_i = 108/(12.6)^2 \quad = 0.7°$$
$$\delta = \cos(\theta_o + \theta_i) = \cos 0.7° \simeq 1.0$$
$$20 \log \delta = 0 \text{ dB.}$$

From Figure 5 and equation (6), we can expect scintillation (atmospheric and iono-spheric) to provide a standard error in elevation angle of the order of

$$S'(\varepsilon - \varepsilon_o) = 0.0036 \, [1 + (0.3/12.6)^2]^{1/2}$$
$$= 0.0036 \, (1.00028) \simeq 3.5(10)^{-3} \text{ degrees.}$$

We determined from Figure 9 that the aforementioned CPA values for $f = 12.6$ GHz and $\varepsilon = 30°$, $A(p,30°)$, were exceeded for the indicated p percent of the hours during 99 out of 100 years. The corresponding received signal power exceeded for $100 - p$ percent of all hours (or for all but p percent of the hours) in 99 out of 100 years is given by (15b)

$$P_R(100 - p) = P_T - L_o - A(p,30°)$$
$$= 0 - 99.02 - A(p,30°).$$

Therefore

$$P_R(50\%) \quad = -99.02 - 1.1 \ = -100.12 \ \text{ dBW}$$
$$P_R(99.55\%) = -99.02 - 1.7 \ = -100.72 \ \text{ dBW}$$
$$P_R(99.9\%) \ = -99.02 - 6.82 = -105.84 \ \text{ dBW}$$
$$P_R(99.99\%) = -99.02 - 17.7 = -116.72 \ \text{ dBW}$$

The associated signal-carrier-to-noise ratio in decibels is given by

$$(c/n)_{dB} = P_R(100 - p) - N(p)$$

For 99.55% of the time

$$(c/n)_{dB} = -100.72 + 125.37 = 24.65 \text{ dB}$$

For 99.9% of the time

$$(c/n)_{dB} = -105.84 + 124.37 = 18.53 \text{ dB}$$

For 99.99% of the time

$$(c/n)_{dB} = -116.72 + 124 = 7.28 \text{ dB}$$

which does not achieve the 15 dB required at $p = 0.01\%$. However, note that if site diversity is employed, Figure 9 indicates that for a site separation of 20 km, the individual site attenuation $A(p_1 = 0.1\%, 30°) = 6.82$ dB would not be exceeded for $p_2 = 0.01\%$. Further, for the joint probability $p_2 = 0.01\%$, $N = N(p_1 = 0.1\%)$.

Then, for $100 - p_2 = 99.99\%$

$$
\begin{aligned}
(c/n)_{dB} &= P_T - L_o - A(0.1\%, 30°) - N(0.1\%) \\
&= -99.02 - (6.82) - (-124.37) \\
&= -99.02 + 117.55 = 18.53,
\end{aligned}
$$

which meets the requirement $(c/n)_{dB} \geq 15$ dB at $p_2 = 0.01\%$. Note that the site diversity "gain" is

$$
\begin{aligned}
(c/n)_{dB} &= 18.53 - 7.28 = 11.25 \\
&= \delta A(0.01\%) - \delta N(0.01\%) \\
&= A(p_1) - A(p_2) - [N(p_1) - N(p_2)] \\
&= 17.7 - 6.82 - [-124.37 + 124] \\
&= 10.88 + 0.37 = 11.25 \; .
\end{aligned}
$$

Of course, the diversity "advantage" is $p_1/p_2 = 0.1\%/0.01\% = 10$. Similarly, the new attenuation and noise for the joint probability $100 - p_2 = 99.9\%$ is (from Figures 8 and 9 where for $p_2 = 0.1\%$, $p_1 - 0.45\%$), respectively, $A(0.45\%, 30°) = 1.7$ dB and $N(0.45\%) = -125.37$ so that

$$(c/n)_{dB} = -99.02 - 1.7 + 125.37 = 24.65 \text{ dB} \quad .$$

4.0 SYSTEM FIGURES OF MERIT

In telecommunication system design, a figure of merit is a measure of the expected system performance. The desired system performance is, of course, that received signal behavior that achieves the required reliability of information transfer (maximum permissible bit-error rate, minimum acceptable articulation index, etc.). This normally occurs whenever the received carrier-to-noise ratio (c/n) exceeds a specified level. This (c/n) ratio is determined by, and expressed in terms of, the path geometry, propagation factors, and system parameters, as described below. For earth-space systems, this (c/n) figure of merit also has other associated figures of merit, such as the receiving antenna figure of merit (g/T).

The problem of system design, therefore, is that of achieving the specified value for the appropriate figure of merit within the constraints imposed by costs, equipment availability, and the limitations placed on certain system parameters by the radio regulators. For example, to avoid undue intersystem interference, some limits have been placed upon the equivalent isotropically radiated power (e.i.r.p.) and the transmitter power (and antenna gain). The Radio Regulations [ITU, 1976a] limit the e.i.r.p. of terrestrial terminals (earth stations) that is directed toward their horizons (at $\varepsilon = \varepsilon_h$). Although there are exceptions, the general limits on the e.i.r.p. at ε is:

    (a) in the frequency range $1 \leq f \leq 15$ GHz for any 4 kHz band,

$$40 \text{ dBW} \quad \text{for} \quad \varepsilon \leq 0°$$
$$3\varepsilon + 40 \text{ dBW} \quad \text{for} \quad 0 < \varepsilon \leq 5°;$$

    (b) in the frequency range $f > 15$ GHz for any 1 MHz band,

$$64 \text{ dBW} \quad \text{for} \quad \varepsilon \leq 0°$$
$$3\varepsilon + 64 \text{ dBW} \quad \text{for} \quad 0° < \varepsilon \leq 5° \quad .$$

4.1 Power Flux Density

At a distance from the transmitting antenna (r in kilometers), the power flux density is

$$W = 10 \log \frac{P_T \, g_T \delta^2}{4\pi \, a^2 r^2} \quad dBW/m^2, \tag{18a}$$

$$= P_T + G_T - 20 \log r + 20 \log \delta - 71 - CPA \quad dBW/m^2, \tag{18b}$$

for the co-polarized field. The p_T, g_T, P_T, G_T, and $A(p,\epsilon)$ = CPA are as defined in (1), (2), (14), and (15). Also CPA = 10 log a. An associated quantity is the power flux spectral density

$$\Psi = W - 10 \log Bw \quad dBW/m^2 Hz , \tag{19}$$

where B is the system's pre-detection bandwidth in Hertz. Of interest for earth-space systems is the resulting power flux density (PFD) over a specific bandwidth, Bw´ in Hertz,

$$PFD = W + C + 10 \log (Bw´/Bw) \quad dBW/m^2, \quad . \tag{20}$$

$$= \Psi + C + 10 \log Bw \quad dBW/m^2. \tag{20b}$$

The C is a corrective factor for a non-uniform distribution of signal power over the system bandwidth Bw. For downlinks, the Radio Regulations limit the PFD at the earth's surface; some PFD limits are listed in Table 4 [ITU, 1976b]. For any proposed system with a specified bandwidth B and signal power distribution (from which C above would be determined), the PFD limits (such as in Table 4) can be expressed as the system's maximum permissible power flux density, W, from (18a,b).

4.2 The Signal-to-Noise Ratio

From (1), (2), (10), (15b), and (17a), the received carrier-to-noise ratio may be expressed as

$$(c/n)_{dB} = P_R - 10 \log n = P_R - N \quad dB, \tag{21}$$

$$= P_T + G_T + G_R + 20 \log \delta - 10 \log B + 136.15 - CPA$$

$$- 20 \log r - 20 \log f - 10 \log T \quad dB,$$

where $T = T_e + T_R$.

Table 4. Terrestrial Power Flux Density (PFD) Limits from Satellites, for
Specified Bandwidths

Band GHz			Bandwidth Bw' in Hertz	Downlink * dBW/m^2
1.69	to	1.70	$1.5 (10)^6$	-133
1.670	to	2.535	$4.0 (10)^3$	-144 to -154
2.50	to	2.69	$4.0 (10)^3$	-137 to -152
3.40	to	7.75	$4.0 (10)^3$	-142 to -152
8.025	to	11.700	$4.0 (10)^3$	-140 to -150
12.50	to	12.75	$4.0 (10)^3$	-138 to -148
17.7	to	22.0	$1.0 (10)^6$	-150 to -115

* The left-hand limit is for $25° < \varepsilon < 90°$; the right-hand limit is for
$0° \leq \varepsilon \leq 5°$. See ITU [1976b] for further details.

In earth-space systems one commonly encounters the receiving-system figure
of merit, g_R/T, or

$$(g_R/T)_{dB} = G_R - 10 \log T \ . \tag{22}$$

Similarly, there is the earth-space system figure of merit, c/T, or

$$(c/T)_{dB} = P_R - 10 \log T \ , \tag{23}$$

which is related to the carrier-to-noise ratio by [ITT, 1969]

$$(c/n)_{dB} = (c/T)_{dB} + 228.6 - 10 \log B \quad dB. \tag{24}$$

Combining (10), (21), (22), and (23), one may write

$$(c/T)_{dB} = W + (g_R/T)_{dB} - 21.46 - 20 \log f \quad dB \tag{25}$$

or

$$(c/n)_{dB} = W + (g_R/T)_{dB} + 207.14 - 10 \log Bw - 20 \log f \quad dB. \tag{26}$$

Note that these expressions relate the system figures of merit, (c/n) or (c/T), to the power flux density limit, W, adjusted to meet the PDF, and the receiving system figure of merit, (g/T).

4.3 Numerical Examples for Figures of Merit

Turning again to the earth-station/synchronous satellite system, ES_1/S_1 of subsections 2.3 and 3.3, we repeat the downlink parameters

$$P_T = 0 \text{ dBW} \qquad G_S = 48.35 \text{ dBi} \qquad G_{ES} = 58.81 \text{ dBi}$$
$$\delta = 1.0 \qquad C = 0 \qquad f = 12.6 \text{ GHz}$$
$$T(0.1\%) = 665°K \qquad T(0.01\%) = 720°K \qquad T(0.45\%) = 529°K$$
$$A(0.1\%,30°) = 6.82 \text{ dB} \quad A(0.01\%,30°) = 17.7 \text{ dB} \quad A(50\%,30°) = 1.1 \text{ dB}$$
$$L_0 = 99.02 \text{ dB} \qquad Bw = 4(10)^7$$

From (18a), the power flux density at the receiving (ES_1) site is

$$W(100 - p) = 0 + 48.35 - 20 \log (38,568) + 20 \log (1.0) - A(p,30°) - 71 \text{ dBW/m}^2$$
$$= -114.37 - A(p,30°).$$

Therefore,

$$W(50\%) = -114.37 - 1.1 \quad = -115.47 \quad dBW/m^2$$
$$W(99.99\%) = -114.37 - 17.7 \quad = -132.07 \quad dBW/m^2$$

for non-diversity. For a diversity separation of 20 km such that the $p_2 = 0.01\%$, attenuation is reduced to the single-site value for $p_1 = 0.1\%$

$$W(99.99\%) = -114.37 - 6.82 \quad = -121.19 \quad dBW/m^2.$$

The power flux spectral density at the surface is, from (9),

$$\Psi(100 - p) = W(100 - p) - 10 \log (4 \cdot 10^7)$$
$$= W(100 - p) - 76.02 \quad dBW/m^2Hz.$$

It's maximum value (for $\varepsilon = 90°$ and $100 - p \geq 50\%$) is

$$\Psi(50\%) = -114.37 - 1.1 \quad (0.5) - 76.02 = -190.94 \quad dBW/m^2Hz.$$

From (20b) for $C = 1$,

$$PFD = 190.94 + 10 \log 4(10)^3$$
$$= 190.94 + 36.02 = -154.92 \quad dBW/m^2,$$

which is below the limit of Table 4.

5. INTERFERENCE FOR FREQUENCY ASSIGNMENT AND FREQUENCY SHARING

The foregoing Sections 3 and 4 treated the role of propagation and the environment in achieving a required service reliability. This consisted of providing a service field, a field exceeding a minimum permissible level for at least a specified (90, 99, 99.9, or 99.99) percent of all hours. An associated concern is the toleration of significant inter-system interference between co-channel stations for less than some specified (10, 1, 0.1, or 0.01) percent of all hours. This latter is of immediate concern to the frequency-assignment problem (where the two stations are in the same service) and to the frequency-sharing problem (for which the two stations are not in the same service).

5.1 The Signal-to-Interference Ratio

Consider either of the (receiving) terminals of a slant-path system. From (1), (15a), and (15b), the desired-signal received power is given by

$$P_R = P_T - L = P_T - L_0 - A(p,\varepsilon) \quad dBW,$$
$$= P_T + G_T + G_R + 20 \log \delta - L_{bo} - A(p,\varepsilon) \quad dBW, \tag{27}$$
$$= P_T + G_T + G_R + 20 \log \delta - 92.45 - 20 \log f - 20 \log r - A(p,\varepsilon) \quad dBW.$$

Here, L is the transmission loss for the <u>service propagation path</u> and P_T, $A(p,\varepsilon)$, etc., are as previously defined. There is, of course, a similar expression for the undesired-signal (interference) received power.

$$
\begin{aligned}
I_R &= P_{Ti} - L_i = P_{Ti} - L_{0i} - A_i(p,\varepsilon) \quad \text{dBW,} &(28)\\
&= P_{Ti} + G_{Ti}(\Delta_T) + G_{Ri}(\Delta_R) + 20\log\delta_i - L_{boi} - A_i(p,\varepsilon) \quad \text{dBW,}\\
&= P_{Ti} + G_{Ti} + G_{Ri} + 20\log\delta_i - 92.45 - 20\log f - 20\log d - A_i(p,\varepsilon) \quad \text{dBW.}
\end{aligned}
$$

Here, L_i is the transmission loss for the interference propagation path and P_{Ti}, δ_i are quantities defined as previously, but with the subscript i added to identify the values appropriate to the interference source. Further:

$G_{Ti}(\Delta_T)$ is the interference source's effective transmitting antenna gain in dBi in the direction Δ_T (relative to the main beam axis) of the interference victim receiver;

d is the interference path length in kilometers; and

$A_i(p,\varepsilon)$ is the interference propagation path transmission loss in excess of the interference path's free-space loss. For the interference path only, the value p = 50% is generally used.

Combining (27) and (28), we determine the signal carrier-to-interference ratio in decibels as

$$
\begin{aligned}
(c/i)_{dB} &= P_R - I_R &(29)\\
&= P_T - P_{Ti} + G_T - G_{Ti} + G_R - G_{Ri}\\
&\quad + 20\log(\delta/\delta_i) + 20\log(d/r) + A_i(p,\varepsilon) - A(p,\varepsilon) \quad \text{dB.}
\end{aligned}
$$

In today's crowded spectrum, this signal carrier-to-interference ratio is increasingly the more important figure-of-merit than those of Section 4.

From a satellite, the interference path will have a directional angle Δ_T or Δ_R in degrees (relative to the satellite's main beam center) given by

$$
\cos\Delta_S = \sin\phi\sin\phi_i + \cos\phi\cos\phi_i\cos\delta B \tag{30a}
$$

where

$$
\delta B = B - B_i.
$$

These parameters ε and ϕ are as previously defined, the i subscript identifies those parameter values appropriate to the interference propagation path. The unsubscripted quantities are those for the service propagation path. There is a similar expression for the earth-station.

$$\cos \Delta_{ES} = \sin \varepsilon \, \sin \varepsilon_i + \cos \varepsilon \, \cos \varepsilon_i \, \cos \delta A, \tag{31a}$$
where
$$\delta A = A - A_i \tag{31b}$$

For the purposes of evaluating a potential for interference, the G'_{Ti} or G'_{Ri} can be determined from available CCIR patterns for satellites of the fixed satellite service and earth-stations in the range $2 \leq f \leq 10$ GHz. The satellite antenna reference pattern (G'_{Ti} or G'_{Ri}) can be expressed for $\Delta \leq 180°$ [CCIR, 1978i; Morgan, 1979] as

$$
\begin{aligned}
G'_S(\Delta) &= G'_0 - 3 \, (\Delta/\Delta_0)^2 \text{ dBi}, & 0 &\leq \Delta/\Delta_0 < 2.6, \\
&= G'_0 - 20 \text{ dBi}, & 2.6 &\leq \Delta/\Delta_0 < 6.3, \\
&= G'_0 - 25 \log (\Delta/\Delta_0) \text{ dBi}, & 6.3 &\leq \Delta/\Delta_0 < 10^m, \\
&= -10 \text{ dBi}, & 10^m &< \Delta/\Delta_0 \leq 180/\Delta_0 .
\end{aligned}
\tag{32a}
$$

Here, G'_0 is the main-beam gain. For a halfpower beamwidth of Ω in degrees,

$$m = (G'_0 + 10)/25 \qquad \text{and} \qquad \Delta_0 = \Omega/2 .$$

For earth stations, the reference off-axis gains have been only partially specified [CCIR, 1978j; Morgan, 1979], as

$$G'(\Delta) = 52 - 25 \log \Delta - 10 \log n \geq -10 \text{ dBi}, \quad \Delta_2 \leq \Delta \leq 180°, \tag{33a}$$
where
$$
\begin{aligned}
n &= 100 \text{ and } \Delta_2 = 1° & &\text{for } D/\lambda \geq 100, \\
&= D/\lambda \text{ and } \Delta_2 = 100 \, \lambda/D & &\text{for } D/\lambda \leq 100.
\end{aligned}
\tag{33b}
$$

However, from Table 2 for a dish antenna with efficiency $\eta = 0.65$ and the expression

$$D/\lambda = Df/0.3 , \tag{34a}$$

one can determine

$$G_0' = G'(\Delta = 0) = 8.07 + 20 \log (D/\lambda) \quad \text{dBi}, \tag{34b}$$

$$10 \log (\Delta_0 = \Omega/2) = 16.03 - 10 \log (D/\lambda) \quad \text{dBi}. \tag{34c}$$

From the foregoing and $G'(\Delta) = G_0' - \Delta G$, one derives

$$
\begin{aligned}
\Delta G_{ES} &= 3 \ (\Delta/\Delta_0)^2 & 0 &\le \Delta/\Delta_0 \le (\Delta/\Delta_0)_1 \\
&= \Delta G_2 & (\Delta/\Delta_0)_1 &\le \Delta/\Delta_0 \le (\Delta/\Delta_0)_2 \\
&= 25 \log (\Delta/\Delta_0) + Q & (\Delta/\Delta_0)_2 &\le \Delta/\Delta_0 \le 10^S \\
&= G_0' + 10 & 10^S &\le \Delta/\Delta_0 \le 180°/\Delta_0
\end{aligned}
\tag{35a}
$$

where

$$s = [G_0' + 10 - Q] / 25$$

$$Q = 10 \log n - 3.85 - 5 \log (D/\lambda) \tag{35b}$$

$$(\Delta/\Delta_0)_1 = (\Delta G_2/3)^{1/2}$$

and for n and Δ_2 given by (33b)

$$
\begin{aligned}
\Delta G_2 &= G_0' - 32 & \text{for } D/\lambda &\ge 100 \ , \\
&= 9.93 + Q & \text{for } D/\lambda &\le 100 \ .
\end{aligned}
\tag{35c}
$$

The off-axis gain reduction patterns ΔG_S and ΔG_{ES} are shown in Figures 10 and 11.

5.2 Potential Interference Fields

For the propagational aspect of the interference problem, it is convenient to consider the potential <u>interference paths</u> between <u>pairs</u> of co-channel stations. This pair consists of one station from each of two systems (in the same or different services);

(a) <u>both of which are on-or near the surface</u>; e.g., one of which is an earth-station (ES_j of either of the Fixed- or Mobile-Satellite Services or of the Space Research Service) and the other of which is a terrestrial station (T_j of either of the Broadcasting, Fixed, or Mobile Services. This pair, ES_j/T_j, constitutes a potential <u>terrestrial interference path.</u>
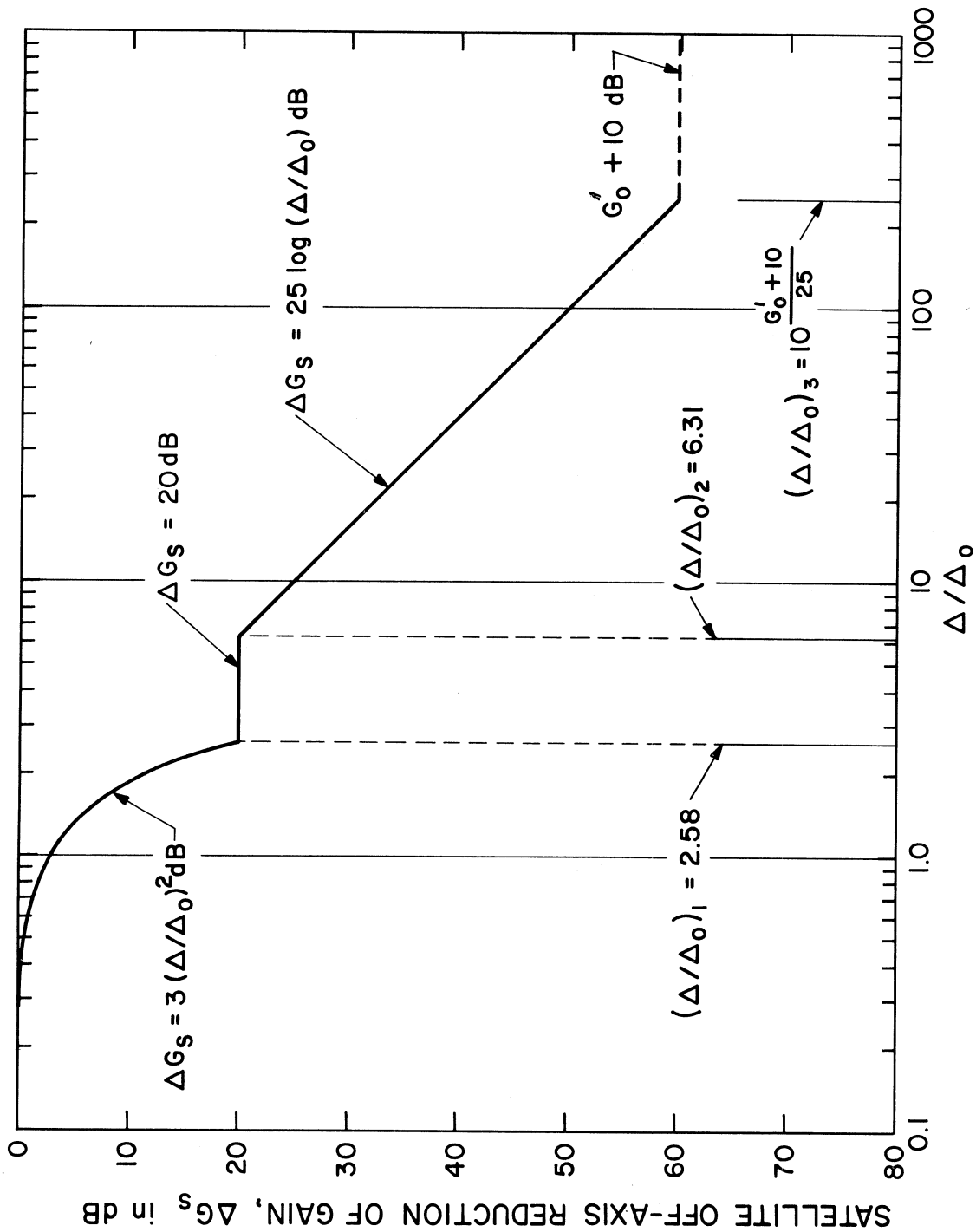
Figure 10. Reference satellite antenna patterns for assessing potential slant-path interference. The off-axis gain $G'(\Delta/\Delta_0)$ is given by the man-lobe gain G'_0, less the off-axis reduction ΔG given above. [CCIR, 1978i;].
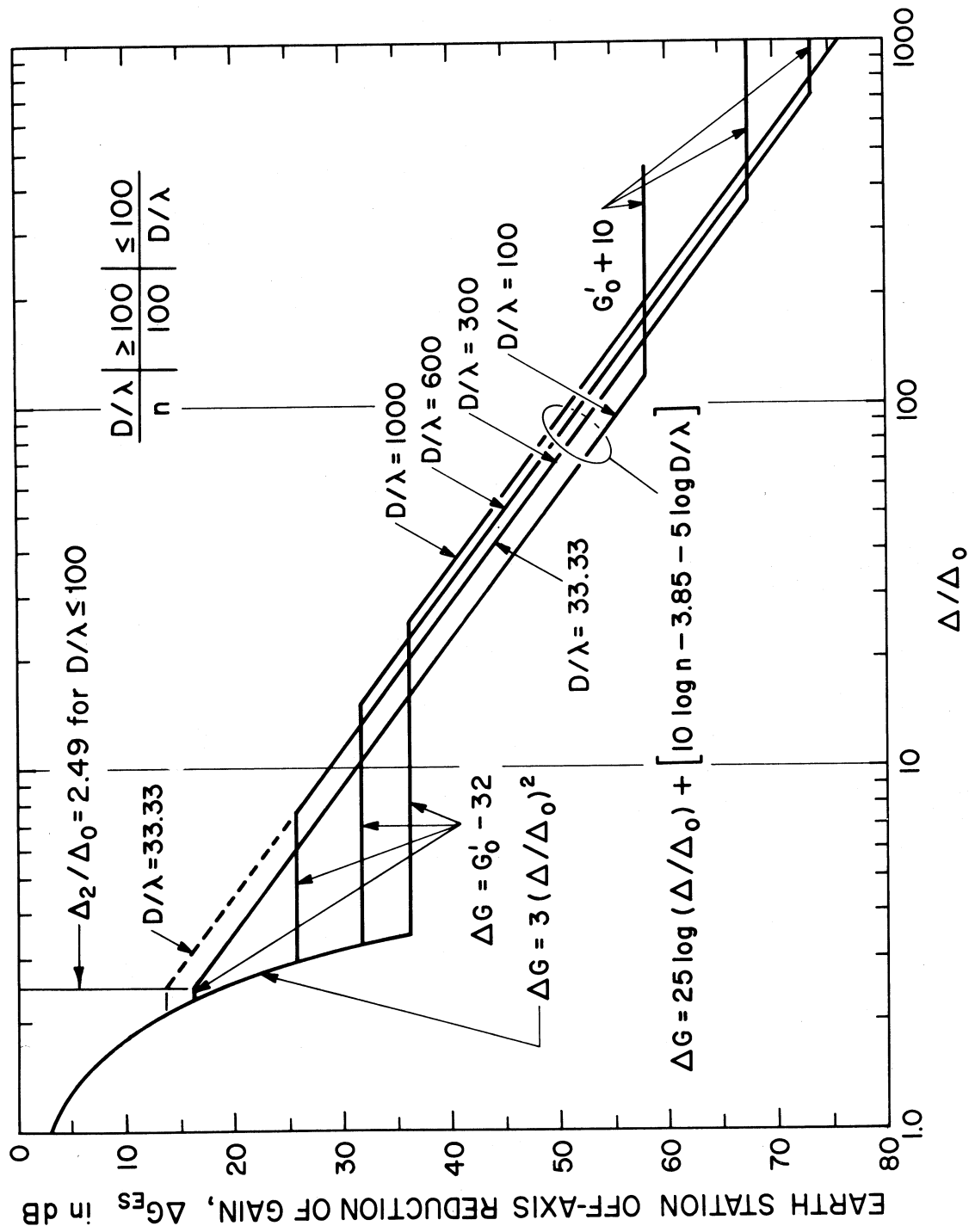
Figure 11. Reference earth-station dish antenna patterns ($\eta = 0.65$) for assessing potential slant-path interference. The off-axis gain $G'(\Delta/\Delta_0)$ is given by the main-beam gain G'_0 less the off-axis gain reduction ΔG given above.

(b) <u>both of which are space stations</u>; e.g., either of which is a Satellite (S_j of the Broadcasting-, Fixed-, or Mobile-Satellite Services) or a space probe (of the Space Research Service). This pair, S_j/S_k, constitutes a potential <u>space/space interference path</u>. Note $j \neq k$.

(c) <u>one of which is on or near the surface</u> ES_j or T_j as in (a) above, <u>and</u> <u>the other of which is a space station</u> S_j as in (b) above. This pair, ES_j/S_k or T_j/S_k, constitutes a <u>slant-path interference path</u>.

Some examples of such interference paths for inter-service pairs are illustrated in Figure 12 from a 1979 NTIA Technical Memorandum report 79-19, Propagational Aspects of Frequency Allocation and Frequency Sharing by H. T. Dougherty and C. M. Rush of the NTIA/ITS staff in Boulder, Colorado.

5.2.1 Terrestrial Interference Paths

The (a) pair above defines the terrestrial interference paths between the earth-station ES_1 on or near the surface and other terminals, T_j or ES_k on or near the surface. For standard propagation conditions, one requires that the interference propagation path be transhorizon to other earth-stations, and also that ES_1 is well beyond the service area of terrestrial stations. However, for small percentages of the time, interference may occur by four modes [CCIR, 1978k]:

(1) by diffraction over short paths for 1 percent to 20 percent of the time;

(2) by tropospheric forward scatter (troposcatter) which would dominate at greater distances than (1), but not for much less than 1 percent of the time;

(3) by hydrometeor (rain, snow, hail, ice clouds) forward-, side-, or back-scattering from antenna main- or side-lobe intersections on or off the great-circle path for less than 1 percent of the time; and

(4) by tropospheric ducting for 1 percent or less of the time as a function of climatic zone, whether the path is over land or over water, temperate or tropic, and for maximum distances over which ducts can extend.

For each of these modes, the interference propagation path loss may be evaluated for the determination of a coordination distance [CCIR, 1978k]. At present, such procedures are specified in the Radio Regulations [ITU, 1976a and b] for possible earth-station/terrestrial station interference; their modification continues under
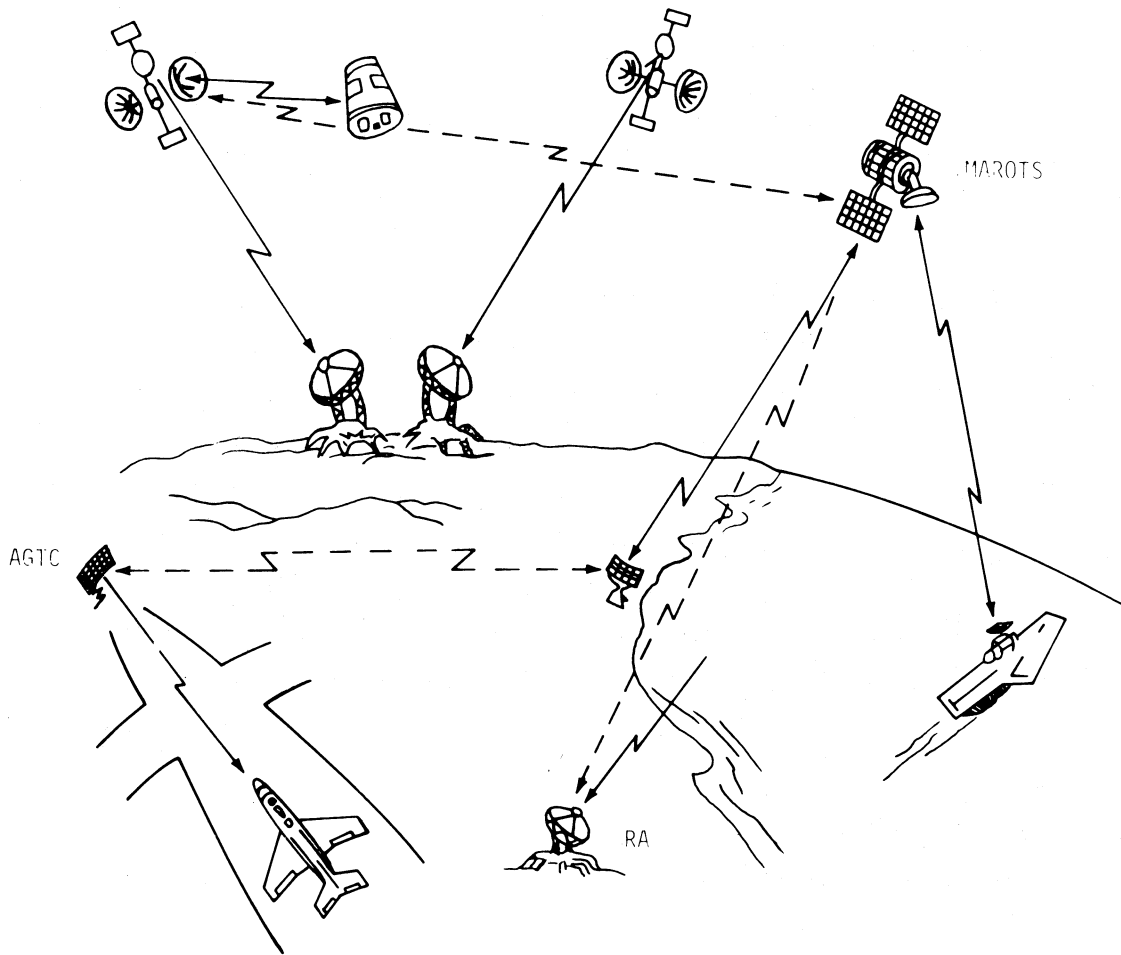
Figure 12.   Some Terrestrial and Space Systems (solid-line service
             signals) with potential interservice interference (dashed-
             line) paths.

consideration by the CCIR as a result of directives from the General World Radio Administrative Conference (GWARC-1979).

5.2.2 Space/Space Interference Paths

For the (b) pair above, interference can arise between satellites whose (main- or side-lobe) antenna beams are directed towards earth-stations and other satellites. This is illustrated by the solid-line propagation paths, indicated in Figure 13, where the antenna patterns (G_j) provide a degree of discrimination. Generally, these interference paths are beyond the earth's atmosphere so that free-space propagation would apply. Note, however, that the broad-beam coverage of S_3 and the spot-beam coverage of S_4 toward the limb of the earth, could permit unusual interference paths to S_1; atmospheric ducting may provide these efficient interference paths to and from the satellites S_3 and S_4 normally isolated from S_1 by the intervening limb of the earth. Then, the transmission loss could approach within 6 dB of that from either satellite to its earth station; therefore, the interference field power flux density at the victim satellite would approach to within 6 dB below the interference source's PFD at the earth's surface.

5.2.3 Slant-Path Interference Paths

The (c) pair determines an interference propagation path that is similar to the service propagation path, differing only because of the location of the transmitting terminal and localized atmospheric conditions along the path. See Figure 14. When estimating the expected signal-to-interference ratio, the major difference in evaluating each path is to consider:

    (a). the service propagation path under its most unfavorable conditions; e.g., attenuation losses and depolarization due to atmospheric effects for small percentages of the time (p = 1 percent, 0.1 percent, 0.01 percent)

and (b) the interference propagation path under its most favorable conditions; e.g., the relatively minor atmospheric losses encountered for large percentages of the time ($p \geq 50$ percent) for co-polar interference. Alternately, if the interference source is cross-polarized, the severe attenuation loss that may generate its co-polar component would be of interest.

5.3 Role of Polarization

The potential for the discriminating reception (in favor) of the desired (service) signal and (adverse to) the undesired (interference) signal is most commonly based upon:
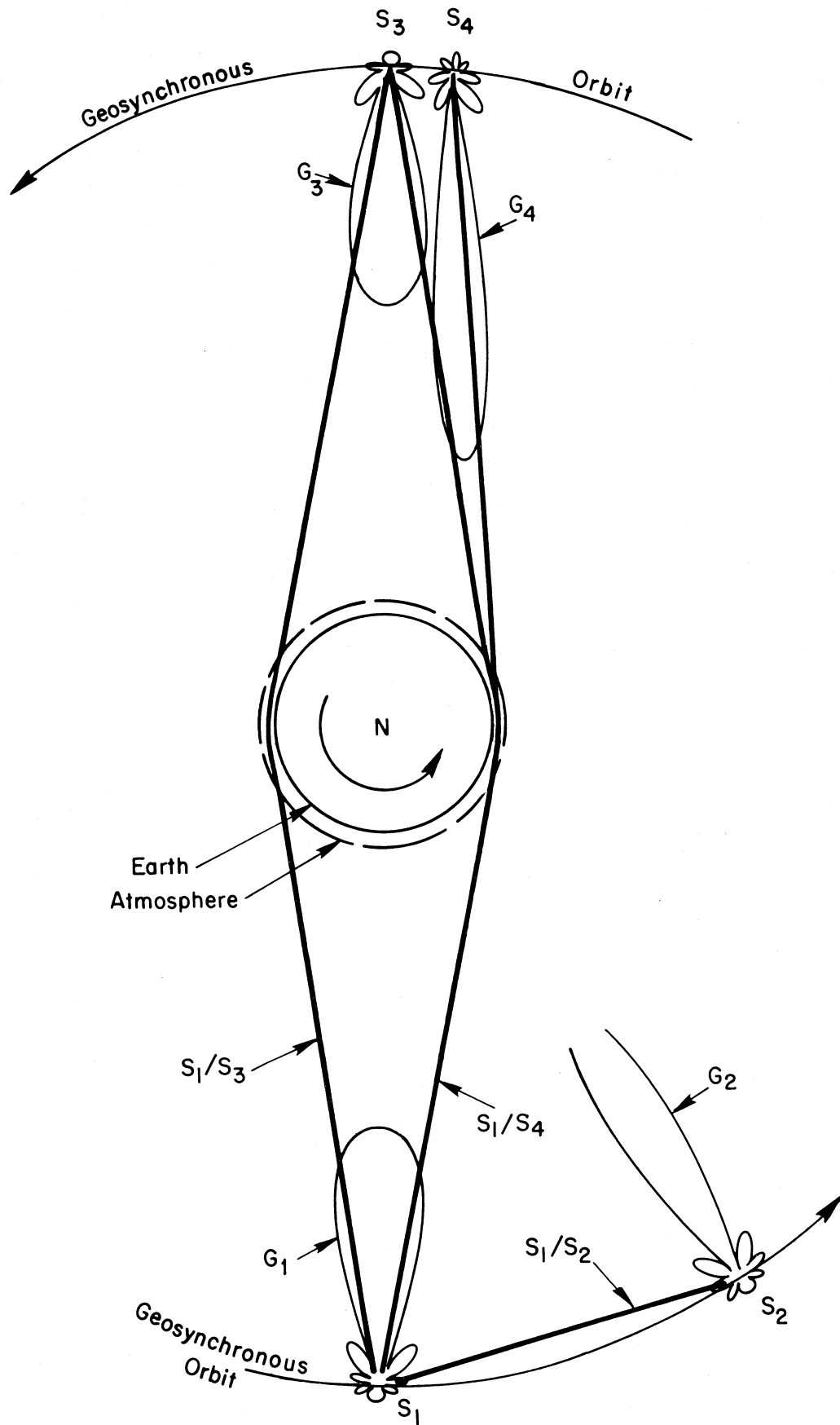
Figure 13.   Satellite-to-satellite interference paths.

(a) antenna pattern discrimination, which exploits the difference in direction of arrival of the service and interference signals, the $(G_R - G_{Ri})$, etc., of (29);

(b) signal polarization discrimination, which exploits any orthogonality between linearly-polarized service and interference signals or the opposite-sense of circularly-polarized service and interference signals;

(c) frequency discrimination, which exploits any frequency separation between the service and interference signals;

(d) bandwidth discrimination, which exploits spread-spectrum techniques;

and **(e) other signal-processing techniques.**

In this subsection, we are concerned only with (b) above.

For the radio regulator, interference is an inter-system, and possibly an inter-service, problem. The implication then is that the transmitting facilities (the desired-signal source and the interference signal source) are separate, not co-locational. The service propagation path and the interference propagation path are then separate, so that their definitions of linear polarization will differ to some degree.

5.3.1 Effects of Geometry

Recall from Section 2.2 that, in the absence of any depolarization effects of the atmosphere, there was still a geometrical effect to be considered:

o   the definitions of linear orthogonal polarization for slant-path systems undergo a **rotation by an angle** θ_o relative to any individual system's definition;

o   the angle of tilt is simply related by a coefficient α to the disparity between systems of δA, their azimuths (ES to SS) and δB, their back azimuths (SS to ES).

$$\theta_o = \delta B - \alpha \cdot \delta A \qquad\qquad (36)$$

The geometry involved in evaluating the potential for interference is illustrated in Figure 14, where one potential interference path between two systems (ES_1/S_1 and ES_2/S_2 or ES_2/SS_2) and its great-circle projection are dashed. The associated θ_o is illustrated in Figures 15 and 16 and in extensions of Figure 4, and the coefficient α is plotted in Figure 16 as a function of δA, δB, and Z_i [Appendix B]. There, we note that for an antenna oriented (pointed) along its service propagation path, it will receive linearly polarized signals from along its interference propagation path that appear to have been rotated an angle θ_o from its (initially defined) transmitted polarization. This can have several implications:
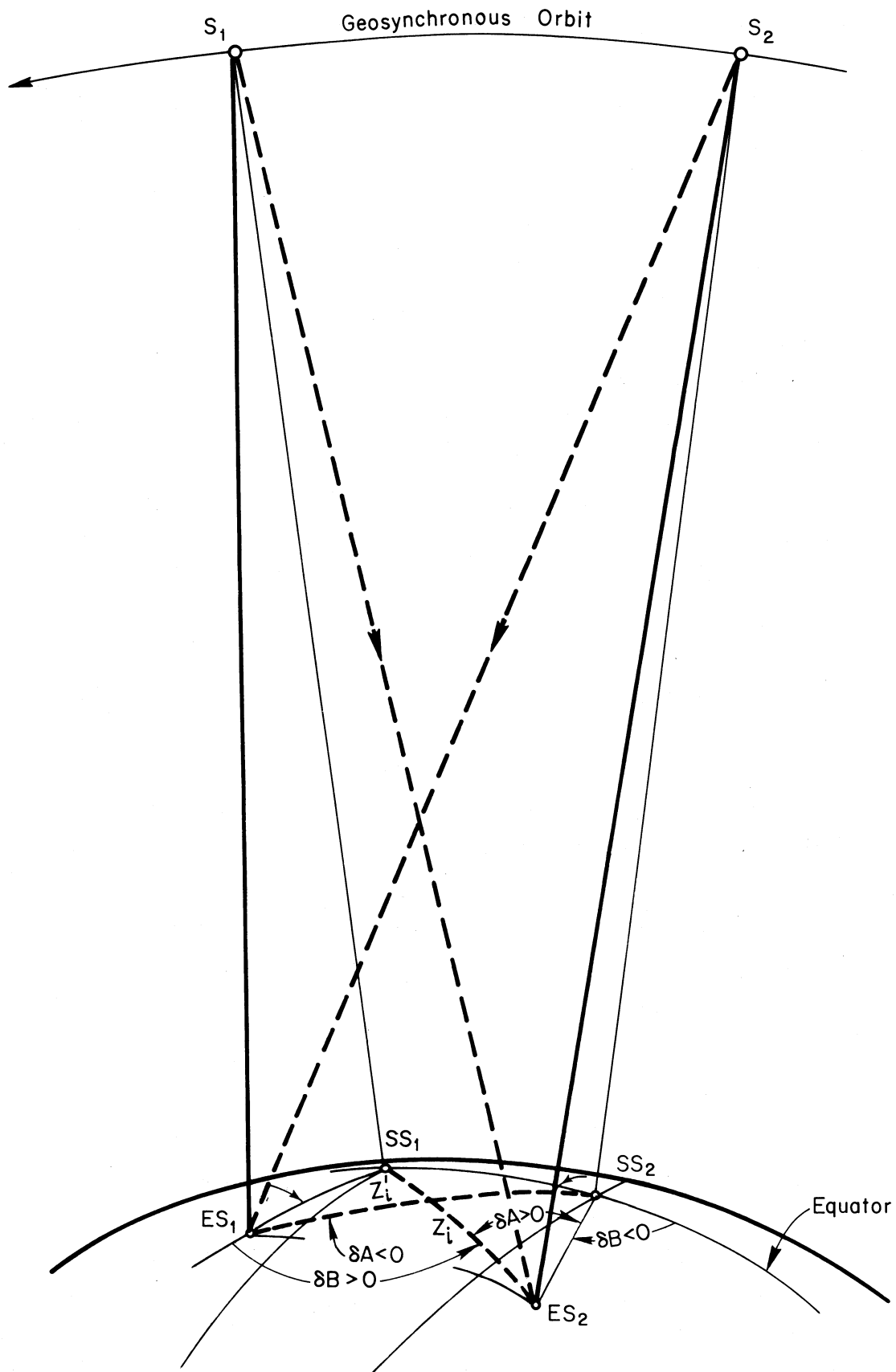
Figure 14. Earth/Space interference paths (dashed lines), their great
circle projections, and service paths (continuous lines)
for two systems (ES_1/S_1 and ES_2/S_2).

Figure 15. The depolarization angle for linear polarization due to their disparity of definitions for a potential interference situation.
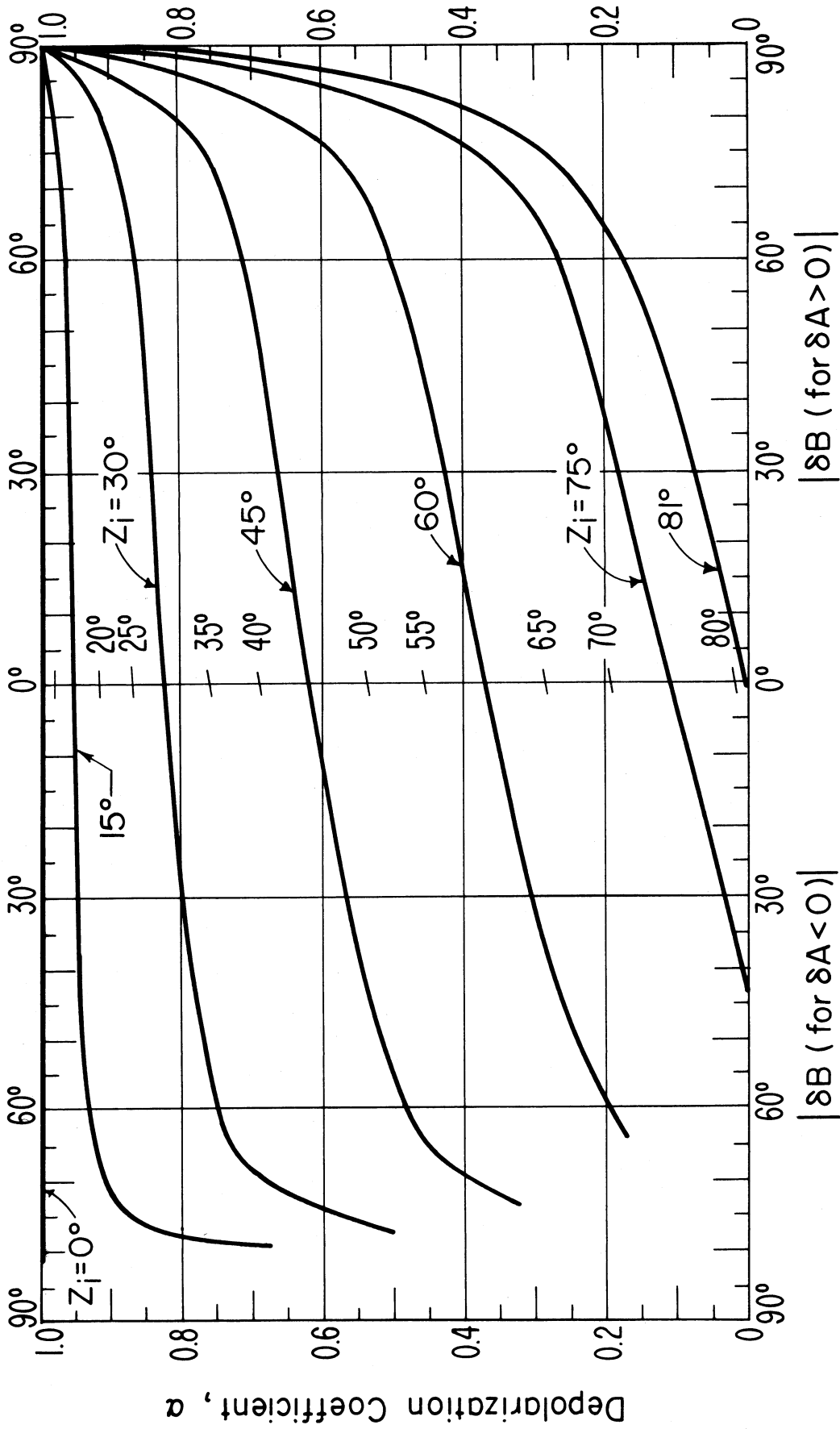
MAGNITUDE OF DIFFERENCE IN BACK-AZIMUTH, $|\delta B|$ in degrees

Figure 16. The depolarization angle coefficient α as a function of the differences in azimuth (δA) and back-azimuth (δB) and the great-circle interference-path project (Z_i).

o   The angular rotation of linear polarization, θ_o, is essentially the same for any orthogonal linear polarization.

o   Since a circularly polarized wave may be considered as the sum of two equal-amplitude, orthogonal, linearly polarized waves, 90° out of time phase, the impact of the disparate definitions of linear polarization is minimal. The signal polarization remains circular over the illuminated earth's surface, lacking the ellipticity that would result if an opposite-sense (cross-polarized) circularly polarized wave were also generated.

As a result, we note that:

o   for two slant-path systems, interference may be reduced by employing opposite-sense circularly polarized signals to or from any part of the visible earth's surface;

o   for two slant-path systems serving small (spot beam) overlapping service areas, interference can be reduced by employing orthogonal polarizations, the XPD and CPA are given by Figure 4.

5.3.2. Atmospheric Effects

In addition to the rotation of linear signal polarization that occurs because of geometry (subsection 2.2.) or from transiting the ionospheric (subsection 3.3.2.), clouds and rainfall also cause a depolarization (i.e., rotation of polarization) of radio waves. For linear polarization, the resulting cross-polarization refers to the orthogonal linear polarization; these are usually spoken of as vertical and horizontal polarization. For circular polarization, depolarization results in a cross-polarization; i.e., opposite-sense polarization. These are usually referred to as left-hand and right-hand circular polarization.

In the case of linear polarization, the rotation generates an orthogonal component, as illustrated in Figure 17 for an initially vertically polarized signal E_T. The co-polarized signal attenuation by rainfall is

$$CPA_r = 20 \log (E_T/y), \quad dB \tag{37a}$$

where y is the attenuated co-polarized component. If we designate the resulting orthogonal component as x, the cross-polarization discrimination XPD would be given by

$$XPD_r = 20 \log (E_T/x) \quad dB. \tag{37b}$$

These are inter-related by the depolarization angle θ_r and

$$XPD_r = CPA_r - 20 \log (\tan |\theta_r|) \quad dB. \tag{37c}$$

This XPD would be a measure of the signal-to-interference ratio generated for a system achieving frequency reuse by means of dual orthogonally polarized channels. This intra-system interference is not of concern here, but the XPD is; it is also a measure of the cross-polarized signal attenuation.

Subsection 3.2 described the prediction of CPA or $A(p,\varepsilon)$ in the presence of rainfall, but prediction of XPD in (37c) is not determinable from the CPA without a knowledge of θ_r. However, measurements of CPA and XPD in the presence of rainfall have established an empirical measure, suitable for prediction purposes [CCIR, 1978a]. That is

$$XPD = U - 20 \log [CPA] \quad dB. \tag{38a}$$

where $\quad U = 30 \log f - 40 \log [\cos \varepsilon] - 20 \log |\sin 2\theta_r| \quad .$ (38b)

Here, $\quad$ f $\qquad$ is the transmission frequency in gigahertz;

$\qquad \varepsilon \qquad$ is the terrestrial-terminal elevation angle;

$\qquad |\theta_r| \qquad$ is the polarization tilt due to rainfall and is taken as 45° for circular polarization; and

$\qquad$ CPA $\qquad$ is the co-polarized signal attenuation in decibels.

The cross-polarization discrimination of (38a) is empirical and, therefore, includes the depolarization effect of both non-spherical raindrops and the elongated ice crystals in clouds. In the absence of rainfall, the ice crystals can still cause significant depolarization, but the associated CPA is then almost negligible below 6 GHz, becoming increasingly important with increasing radio frequency. At EHF, this depolarization by ice crystals may be the dominant effect in rainstorms, but is not of concern here. The CCIR is presently reviewing studies of the empirical relationship between CPA and XPD [CCIR, 1978 1]; some updating of (38a, 38b, and 38c) can be expected soon.

Combining (37c), (38a), (38b), and (38c),

$$40 \log (\cos \theta_r) = 30 \log f - 40 \log (\cos \varepsilon) - CPA - 20 \log CPA - 6.02. \tag{39}$$
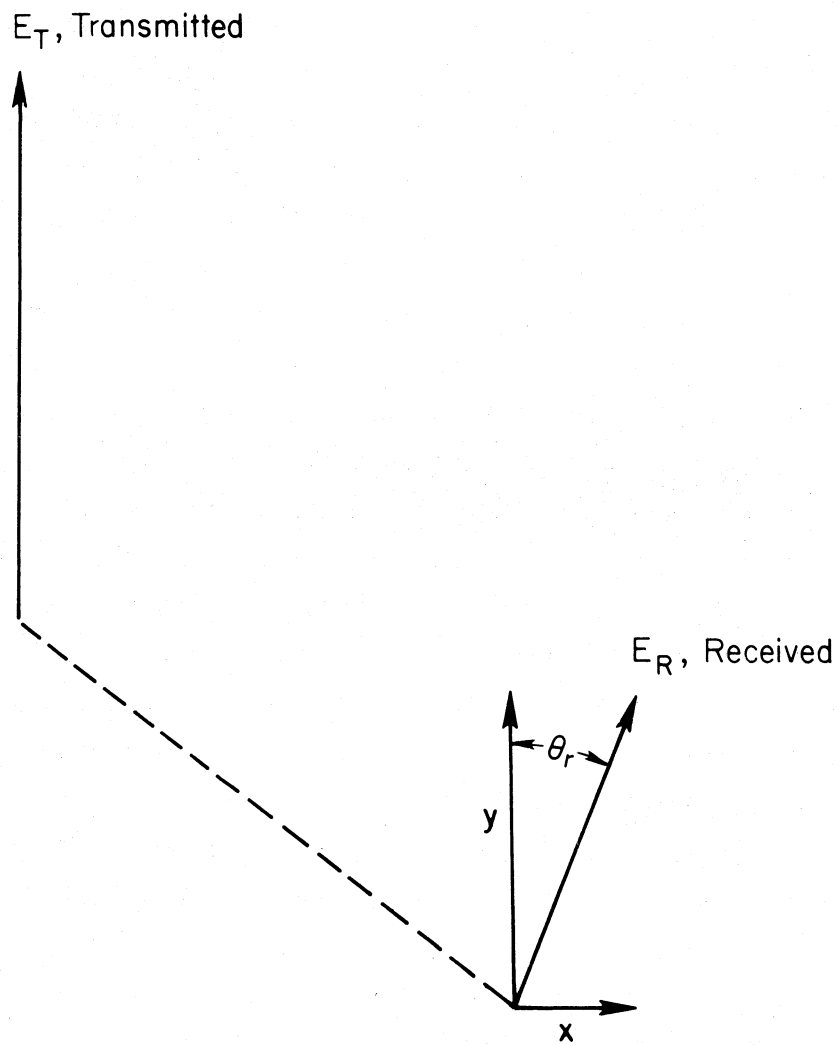
Figure 17. Nomenclature diagram for depolarization by the atmosphere.

This permits a determination of $|\theta_r|$ from the parameters CPA , ϵ, and f. Of course, the total angle of depolarization is

$$\theta = \theta_o + \theta_i + \theta_r ,\qquad\qquad (40)$$

where θ_o, θ_i, and $|\theta_r|$ are determined from, respectively (36), (13), and (39).

5.4 Numerical Examples for Allocation and Sharing

To illustrate the application of the expressions in the previous subsection, let us assume two slant-path systems. One system consists of a satellite S_1 over 77.5°W and an earth-station ES_1 at 38°N and 77.5° west, south of Washington, D. C. A second system will consist of a satellite S_2 over 116°W and an earth-station ES_2 at 43° N and 84°W, north of Detroit and east of Flint, Michigan. Tables 5 and 6 identify the locational parameters (listed in the table's first column), not only for these service paths but also for the associated inter-system potential interference paths. Also listed in the first column is the number of the associated figure or equation from which the listed values were determined. Notice that the antenna-related parameters have different values from those of subsections 2.3., 3.3., and 4.3., because of the different antenna efficiency value $\eta = 0.65$, assumed here. For convenience, we assume that both satellite antennas are 3 m dishes and both earth-station antennas are 10 m dishes. The values for A (0.01%, ϵ) and A (50%, ϵ) were determined for both frequencies and the elevation angles of interest, by the computer program DEGP77 (available from E. J. Dutton of the NTIA/ITS staff in Boulder). For convenience, we have assumed that for both systems, the transmitter power, antennas, and frequencies are the same. This is not uncommon for systems in the same service. The bandwidths are 40 MHz.

From (39) and the values listed in Tables 5 and 6, we can determine for the system ES_2/S_2 and ES_2/S_1 downlinks at 12.2 GHz that

$$\begin{aligned}
CPA &= A\ (0.01\%,\ 30°) = 16.17 \quad dB \\
&= A\ (50\%,\ 40.5°) = 0.8 \quad dB \ .
\end{aligned}$$

From (39) for p = 0.01%,
$$\begin{aligned}
40 \log \cos \theta_r &= 30 \log (12.2) - 40 \log (\cos 30°) - 20 \log (16.17) - 16.17 - 6.02 \\
&= 32.59 + 2.5 - 24.17 - 22.19 = -11.27 \\
\cos \theta_r &= 0.523 \\
\theta_r &= 58.47
\end{aligned}$$

Table 5. Slant-Path Parameter Values for Two Earth-Station/Synchronous-Satellite Systems For a Satellite Spacing of 38.5°, D_{ES} = 10 m, D_S = 3 m

Parameter	Service Propagation Paths				Interference Propagation Paths			
	ES$_1$/S$_1$		ES$_2$/S$_2$		ES$_2$/S$_1$		ES$_1$/S$_2$	
1 L (ES)	38.0° N		43.0° N		43.0° N		38.0° N	
2 ℓ (ES)	77.5° W		84.0° W		84.0° W		77.5° W	
3 ℓ (SS)	77.5° W		116.0° W		77.5° W		116.0° W	
4 δℓ	0.0°		32.0°		-6.5°		38.5°	
5 A (Fig. 3)	180.0°		223.0°		170.0°		233.0°	
6 B (Fig. A3)	0.0°		30.0°		-7.0°		39.0°	
7 Z (Fig. 3)	38.0°		52.0°		43.0°		52.0°	
8 r/R_0 (Fig. 1)	5.855		6.045		5.92		6.045	
9 ε (Fig. 1)	46.0°		30.0°		40.5°		30.0°	
10 φ (Fig. 1)	6.0°		7.4°		6.8°		7.4°	
11 r or d, km	37,343.2		38,555.0		37,757.7		38,555.0	
12 δB (30b)	0.0°		0.0°		7.0°		-9.0°	
13 δA (31b)	0.0°		0.0°		53.0°		-53.0°	
14 α (16)	-		-		0.67		0.54	
15 θ_0 (36)	0.0°		0.0°		-28.51°		19.62°	
16 f, GHz	↓12.2	14.2↑	↓12.2	14.2↑	↓12.2	14.2↑	↓12.2	14.2↑
17 L_{bo}, dB	205.62	206.94	205.94	207.22	205.72	207.04	205.90	207.22
18 A(0.01%,ε) dB	15.45	22.49	16.17	23.45	---	---	---	---
19 A(50%, ε), dB	---	---	---	---	0.8	1.0	1.02	1.49
20 $\lvert\theta_p\rvert$ (39)	46.00	64.52°	58.47°	71.32°	0.0°	0.0°	0.0°	0.0°
21 θ_i (13)	0.73°	0.54°	0.73°	0.54°	0.73°	0.54°	0.73°	0.54°
22 θ_{max} (40)	46.73°	65.06°	59.20°	71.86°	-27.78°	-27.97°	20.35°	20.16°
23 δ = cos θ_{max}	0.685	0.422	0.512	0.311	0.885	0.883	0.938	0.939
24 20 log δ, dB	-3.29	-7.49	-5.81	-10.14	-1.06	-1.08	-0.56	-0.55
25 $G_t + G_r$, dB	108.05	110.68	108.05	110.68	108.05	110.68	108.05	110.68
26 L(0.01%,ε) (27)	116.31	126.24	119.93	130.22	---	---	---	---
27 L_i(50%,ε), dB	---	---	---	---	99 52	98.44	99.43	98.58
28 $L_i - L_i$ dB	---	---	---	---	-20.41	-27.80	-16.88	-31.64
29 Δ_S (30a)	---	---	---	---	7.02°		8.92°	
30 Δ_{ES} (31a)	---	---	---	---	43.86°		39.65°	
31 $(\Delta_0)_S$ (34c)	---	---	---	---	0.33°	0.28°	0.33°	0.28°
32 $(\Delta_0)_{ES}$ (34c)	---	---	---	---	0.10°	0.08°	0.10°	0.08°
33 $(\Delta/\Delta_0)_S$	---	---	---	---	21.27	25.07	27.03	31.86
34 $(\Delta/\Delta_0)_{ES}$	---	---	---	---	438.6	548.25	396.5	495.63
35 ΔG_S, dBi	---	---	---	---	33.19	34.98	35.80	37.58
36 ΔG_{ES}, dBi	---	---	---	---	69.15	71.25	68.06	70.15
37 $\Delta G_S + \Delta G_{ES}$	---	---	---	---	102.34	106.23	103.86	107.73
38 (c/i) dB	---	---	---	---	81.93	78.43	86.98	76.09

Table 6. Effective Antenna Gains* for Two Earth-Station/Synchronous-Satellite Systems

PARAMETER		DOWNLINK		UPLINK	
f		12.2	GHz	14.2	Ghz
D_T		3.0	m	10.0	m
$(D/\lambda)_T$	(34a)	122.0		473.3	
$G_T^{'}$	(34b)	49.8	dBi	61.57	dBi
** G_T		48.8	dB	60.57	dB
$\Omega_T/2$	(34b,c)	0.33°		0.08°	
D_R		10.0	m	3.0	m
$(D/\lambda)_R$	(34a)	406.7		142.0	
$G_T^{'}$	(34b)	60.25	dBi	51.11	dBi
** G_R		59.25	dB	50.11	dB
$\Omega_R/2$	(34b,c)	0.10°		0.28°	
$G_T + G_R$		108.05	dB	110.68	dB
m		2.39		2.44	
Q		3.1	dB	2.77	dB
s		2.69		2.75	

* assuming an efficiency η = 0.65

** assuming line, radome, and pointing losses of 1 dB.

From (37c) for p = 0.01%,

$$XPD = 16.17 - 20 \log (\tan 58.47)$$
$$= 16.17 - 20 \log (1.630)$$
$$= 16.17 - 4.24 = 11.93 \quad dB.$$

The total depolarization for p = 0.01%, assuming all rotations are in the same direction, is

$$\theta = 0 + 0.73 + 58.47 = 59.20$$
$$\delta = \cos 59.2° = 0.512$$
$$-20 \log \delta = 5.81 \quad dB.$$

From (18b), (20a). and Table 5, for C = 1.0 and P_T = 0 dBW, the PFD (50%) is

$$PFD = 0 + 48.8 - 20 \log (37{,}757.7) + 20 \log (\cos 27.78°)$$
$$- 71 - 1.06 + 10 \log (4/40{,}000)$$
$$= -23.26 - 91.54 - 1.06 - 40$$
$$= -155.86 \quad dBW/m^2$$

per 4 kHz of a 40 MHz bandwidth, system.

From (31a) at the receiving ES_2,

$$\cos \Delta_i = \cos \Delta_{ES} = \sin 30° \sin 40.5° + \cos 30° \cos 40.5° \cos 53°$$
$$= 0.5 (0.6494) + 0.8660 (0.7604) 0.6018$$
$$= 0.3247 + 0.3963 = 0.7210$$
$$\Delta_i = \text{arc } \cos (0.7210) = 43.86°.$$

From Table 6 and the above

$$(\Delta_i/\Delta_o)_R = 43.86° /0.10° = 438.6 .$$

From Table 6, (35b)

$$S = \frac{G_0' + 5 \log (406.7) + 13.85 - 20}{25}$$

$$= \frac{60.25 + (13.05) - 6.15}{25} \qquad = \frac{67.05}{25} = 2.69$$

$$10^S = 489.78$$

From Figure 11 or (35a), since $10 < \Delta_i/\Delta_0 = 438.6 < 10^S$

$$\Delta G_{ES} = 25 \log (438.6) + 10 \log (100) - 3.85 - 5 \log (406.7)$$
$$\Delta G_{ES} = -69.15$$

From (30a) at the transmitting S_1

$$\cos \Delta_i = \cos \Delta_S = \sin 6° \sin 6.8° + \cos 6° \cos 6.8° \cos 7°$$
$$= 0.1045 (0.1184) + 0.9945 (0.9930) \, 0.9925$$
$$= 0.0124 + 0.9802 = 0.9925$$
$$\Delta_i = \text{arc cos } (0.9925) = 7.02°$$

From Table 6, (32c), and the above

$$(\Delta_i/\Delta_0)_T = 7.02°/0.33° = 21.27$$

From Table 6 and (32b) and

$$G_0' = 49.8 \quad \text{dBi} \quad ,$$

$$m = \frac{49.8 + 10}{25} = 2.39$$
$$10^m = 245.47 \; .$$

From (32a), since $6.3 < \Delta_i/\Delta_0 << 245$,

$$\Delta G_S = 25 \log (\Delta_i/\Delta_0) = 25 \log (21.27) = 33.19.$$

Therefore

$$\Delta G_T \, (\Delta_i/\Delta_0) + \Delta G_R \, (\Delta_i/\Delta_0) = -33.19 - 69.15$$
$$= -102.34 \text{ dB}$$

From (27) and Table 5 for the ES_2/S_2 system

$$P_R(99.99\%, 30°) = 0 + 108.05 - 5.81 - 206.00 - 16.17$$
$$= -119.93 \quad \text{dBW.}$$

From (36) and (40), for the ES_2/S_1, interference path,

$$\theta = [7 - 0.67 \, (53)] + 0.73 = -27.78°$$
$$\cos \theta = 0.8847$$

and from (28) and Table 5,

$$I_R(50\%, 40.5°) = 0 + 108.05 - \Delta G_T \, (\Delta_i/\Delta_0) - \Delta G_R(\Delta_i/\Delta_0)$$
$$+ 20 \log \delta_i - 205.71 - 0.8$$
$$= -98.46 + 20 \log (0.8847) - 102.34$$
$$= -200.80 - 1.06 = -201.86 \quad \text{dBW.}$$

Therefore

$$P_R(99.99\%, 30°) - I_R(50\%, 42.5°) = (c/i)_{dB} = -119.93 + 201.86 = 81.93 \text{ dB.}$$

This is a comfortable margin, but it is largely due to the antenna pattern discrimination.

Table 7 illustrates the more interesting situation with a reduced earth-station antenna (D = 2m) and the satellite S_2 shifted to 81.5° W for a reduced satellite spacing of 4°. The results are listed in Table 7; the (c/i) values are still adequate.

It has been suggested that interchanging the positions of the satellites would reduce interference. In Table 8, the satellites have been interchanged, as indicated by a spacing of -4.0°. Although this increases the interference signals' depolarization due to geometry (items 15 under ES_1/S_2 in Tables 7 and 8), the net impact upon the new (c/i) values in dB (item 38 in Tables 7 and 8) is slight. The (c/i) values are reduced by an average 1.29 dB for the ES_1/S_2 interference slant-path, but increased by an average 1.24 dB for the ES_2/S_1 interference

Table 7. Slant-Path Parameter Values for Two Earth-Station/Synchronous-Satellite Systems For a Satellite Spacing of 4.0° and Small Earth-Station Antennas, D_{ES} = 2m

	Parameter	Service Propagation Paths ES$_1$/S$_1$		Service Propagation Paths ES$_2$/S$_2$		Interference Propagation Paths ES$_2$/S$_1$		Interference Propagation Paths ES$_1$/S$_2$	
1	L (ES)	38.0°N		43.0°N		43.0°N		38.0°N	
2	ℓ (ES)	77.5°W		84.0°W		84.0°W		77.5°W	
3	ℓ (SS)	77.5°W		81.5°W		77.5°W		81.5°W	
4	δℓ	0.0°		-2.5°		-6.5°		4.0°	
5	A (Fig. 3)	180.0°		176.3°		170.0°		186.4°	
6	B (Fig. A3)	0.0°		-2.7°		-7.0°		5.1°	
7	Z (Fig. 3)	38.0°		43.1°		43.0°		38.2°	
8	r/R$_0$ (Fig. 1)	5.855		5.920		5.92		5.857	
9	ε (Fig. 1)	46.0°		40.3°		40.5°		45.8°	
10	φ (Fig. 1)	6.0°		6.6°		6.8°		6.06°	
11	r or d, km	37,343.2		37,757.8		37,757.7		37,355.9	
12	δB (30b)	0.0°		0.0°		7.0°		-7.8°	
13	δA (31b)	0.0°		0.0°		6.3°		-6.4°	
14	α (Fig. 16)	---		---		0.67		0.69	
15	θ$_0$ (36)	0.0°		0.0°		2.78°		-3.38°	
16	f, GHz	↓12.2	14.2↑	↓12.2	14.2↑	↓12.2	14.2↑	↓12.2	14.2↑
17	L$_{bo}$, dB	205.62	206.94	205.72	207.04	205.72	207.04	205.63	206.95
18	A(0.01%,ε) dB	15.45	22.49	15.8	22.8	---	---	---	---
19	A(50%, ε), dB	---	---	---	---	0.7	1.0	0.7	0.9
20	|θ$_p$| (39)	46.00°	64.52°	52.1°	67.49°	0.0°	0.0°	0.0°	0.0°
21	θ$_i$ (13)	0.73°	0.54°	0.73°	0.54°	0.73°	0.54°	0.73°	0.54°
22	θ$_{max}$ (40)	46.63°	65.06°	52.83°	68.03°	3.51°	3.32°	-2.65°	-2.84°
23	δ = cos θ$_{max}$	0.685	0.422	0.604	0.374	0.998	0.998	0.999	0.999
24	20 log δ, dB	-3.29	-7.49	-4.38	-8.54	-0.02	-0.02	-0.01	-0.01
25	G$_t$ + G$_r$, dB	94.08	96.70	94.08	96.70	94.08	96.70	94.08	96.70
26	L(0.01%,ε) (27)	130.28	140.22	131.82	141.68	---	---	---	---
27	L$_i$(50%,ε), dB	---	---	---	---	112.36	111.36	112.34	111.16
28	L$_i$ - L$_i$ dB	---	---	---	---	-19.46	-28.46	-17.94	-30.52
29	Δ$_S$ (30a)	---	---	---	---	7.00°		7.77°	
30	Δ$_{ES}$ (31a)	---	---	---	---	4.80°		4.46°	
31	(Δ$_0$)$_S$ (34c)	---	---	---	---	0.33°	0.28°	0.33°	0.28°
32	(Δ$_0$)$_{ES}$ (34c)	---	---	---	---	0.49°	0.42°	0.49°	0.42°
33	(Δ/Δ$_0$)$_S$	---	---	---	---	21.21	25.00	23.55	27.75
34	(Δ/Δ$_0$)$_{ES}$	---	---	---	---	9.80	11.43	9.10	10.62
35	ΔG$_S$, dBi	---	---	---	---	33.16	34.95	34.30	36.08
36	ΔG$_{ES}$, dBi	---	---	---	---	27.88	29.22	29.68	31.68
37	ΔG$_{ES}$, Δ	---	---	---	---	61.04	64.17	63.98	67.76
38	(c/i) dB	---	---	---	---	41.58	35.31	46.04	37.24

Table 8. Slant-Path Parameter Values for Two Earth-Station/Synchronous-Satellite Systems For a Satellite Spacing of -4° and Small Earth-Station Antennas, D_{ES} = 2m

Parameter	Service Propagation Paths ES_1/S_1		Service Propagation Paths ES_2/S_2		Interference Propagation Paths ES_2/S_1		Interference Propagation Paths ES_1/S_2	
1 L (ES)	38.0°N		43.0°N		43.0°N		38.0°N	
2 ℓ (ES)	77.5°W		84.0°W		84.0°W		77.5°W	
3 ℓ (SS)	81.5°W		77.5°W		81.5°W		77.5°W	
4 $\delta\ell$	4.0°		-6.5°		-2.5°		0.0°	
5 A (Fig. 3)	186.4°		170.0°		176.3°		180.0°	
6 B (Fig. A3)	5.1°		-7.0°		-2.7°		0.0°	
7 Z (Fig. 3)	38.2°		43.0°		43.1°		38.0°	
8 r/R_0 (Fig. 1)	5.857		5.92		5.920		5.855	
9 ε (Fig. 1)	45.8°		40.5°		40.3°		46.0°	
10 ϕ (Fig. 1)	6.06°		6.8°		6.6°		6.0°	
11 r or d, km	37,355.9		37,757.7		37,757.8		37,343.2	
12 δB (30b)	0.0°		0.0°		7.8°		-7.0°	
13 δA (31b)	0.0°		0.0°		-6.3°		6.4°	
14 α (16)	---		---		0.67		0.69	
15 θ_0 (36)	0.0°		0.0°		12.02°		-11.42°	
16 f, GHz	↓12.2	14.2↑	↓12.2	14.2↑	↓12.2	14.2↑	↓12.2	14.2↑
17 L_{bo}, dB	205.63	206.95	205.72	207.04	206.72	207.04	205.62	206.94
18 A(0.01%,ε) dB	15.45	22.49	15.8	22.80	---	---	---	---
19 A(50%, ε), dB	---	---	---	---	0.8	1.0	0.7	0.9
20 $|\theta_p|$ (39)	46.00°	64.52°	52.4°	67.6°	0.0°	0.0°	0.0°	0.0°
21 θ_i (13)	0.73°	0.54°	0.73°	0.54°	0.73°	0.54°	0.73°	0.54°
22 θ_{max} (40)	46.73°	65.06°	53.13°	68.14°	12.75°	12.56°	10.69	10.88
23 $\delta = \cos\theta_{max}$	0.685	0.422	0.600	0.372	0.975	0.976	0.983	0.982
24 20 log δ, dB	-3.29	-7.49	-4.43	-8.59	-0.22	-0.21	-0.15	-0.16
25 $G_t + G_r$, dB	94.08	96.70	94.08	96.70	94.08	96.70	94.08	96.70
26 L(0.01%,ε) (27)	130.28	140.23	131.87	141.73	---	---	---	---
27 L_i(50%,ε), dB	---	---	---	---	112.66	111.55	112.39	111.30
28 $L_i - L_i$ dB	---	---	---	---	-19.21	-28.68	-17.89	-30.43
29 Δ_S (30a)	---	---	---	---	7.77°		7.00°	
30 Δ_{ES} (31a)	---	---	---	---	4.80°		4.46°	
31 $(\Delta_o)_S$ (34c)	---	---	---	---	0.33	0.28	0.33	0.28
32 $(\Delta_o)_{ES}$ (34c)	---	---	---	---	0.49	0.42	0.49	0.42
33 $(\Delta/\Delta_o)_S$	---	---	---	---	23.55	27.75	21.21	25.00
34 $(\Delta/\Delta_o)_{ES}$	---	---	---	---	9.80	11.43	9.1	10.62
35 ΔG_S, dBi	---	---	---	---	34.30	36.08	33.16	34.95
36 ΔG_{ES}, dBi	---	---	---	---	27.88	29.22	29.68	31.68
37 $\Delta G_S + \Delta G_{ES}$	---	---	---	---	62.18	65.30	62.84	66.63
38 (c/i) dB	---	---	---	---	42.97	36.62	44.95	36.20

59

slant path--a negligible _net_ improvement. This is probably to be expected;
Figure 14 suggests that the geometrical relationships are unchanged, although
the dashed-line versus solid-line coding would be reversed for reversed satellite
positions.

6.0 CONCLUSION

This report presents a composite slant-path model for earth/synchronous-satel-
lite systems at UHF/SHF (0.3 to 30 GHz). The model combines three broad areas
(geometry, environment, and interference potential). Each area has an impact
expressible in terms of terminal and path parameters, as attenuation, depolarization,
and noise or in terms of conventional figures of merit. Explicit engineering
expressions and/or graphs are provided to determine these effects quantitatively.
Their application is illustrated by numerical examples.

The material presented in this report has, for the most part, been gathered
from the open literature. The concern has been to present quantitative information
that is representative without emphasizing its complexity. In most instances, the
data are long standing; in some instances (such as attenuation or depolarization by
rainfall and site diversity), the data are tentative (state-of-the-art) and subject
to updating. The material on the apparent depolarization of radio waves simply by
geometry (i.e., because of disparate definitions) is new, although the problem has
been encountered (partially and indirectly) previously in the literature [Shkarofsky
and Moody, 1976; CCIR, 1978m]. The relatively simple expressions for this depolar-
ization (θ_0) are useful approximations to the very complex spherical geometry of
the appendices.

7. REFERENCES

Bean, B. R., and G. D. Thayer (1959), CRPL exponential reference atmosphere, NBS Monograph 4, Superintendent of Documents, U. S. Government Printing Office, Washington, D. D.

Bean B. R., J. D. Horn, and A. M. Ozmich, Jr. (1960), Climatic charts and data of the radio refractive index for the United States and the world, NBS Monograph 22, November, Superintendent of Documents, U. S. Government Printing Office, Washington, D. C.

Bean B. R., and E. J. Dutton (1968), Radio Meteorology, Dover Publications, Inc., New York, N.Y.

CCIR (1978a), Propagation data required for space telecommunication systems, Report 564-1, Vol. V, Propagation Through Non-Ionized Media, CCIR XIV Plenary Assembly, Kyoto, Japan (NTIS Access No, PB-298-025).*

CCIR (1978b), Report 263-4, Ionospheric effects upon earth-space propagation, Vol. VI, Ionospheric Propagation, CCIR XIV Plenary Assembly, Kyoto, Japan (NTIS Access No. PB-298-026).*

CCIR (1978c), Report 683, Preferred frequency bands for deep-space research using manned and unmanned spacecraft, Annex I, Vol. II, Space Research and Radio Astronomy, CCIR XIV Plenary Assembly, Kyoto, Japan (NTIS Access No. PB-298-022).*

CCIR (1978d), Report 670, Worldwide minimum external noise levels, 0.1 Hz to 100 GHz, Vol. 1, Spectrum Utilization Monitoring, CCIR XIV Plenary Assembly, Kyoto, Japan (NTIS Access No. PB-298-021).*

CCIR (1978e), Report 719, Attenuation by atmospheric gasses, Vol. V, Propagation Through Non-Ionized Media, CCIR XIV Plenary Assembly, Kyoto, Japan (NTIS Access No. PB-298-025).*

CCIR (1978f), Report 720, Radio emission associated with absorption by atmospheric gases and precipitation, Vol. V, Propagation Through Non-Ionized Media, CCIR XIV Plenary Assembly, Kyoto, Japan (NTIS Access No. PB-298-025).*

CCIR (1978g), Report 563-1, Radiometeorological data, Vol. V, Propagation Through Non-Ionized Media, CCIR XIV Plenary Assembly, Kyoto, Japan (NTIS Access No. PB-298-026).*

CCIR (1978h), Report 721, Attenuation and scattering by precipitation and other atmospheric particles, Vol. V, Propagation Through Non-Ionized Media, CCIR XIV Plenary assembly, Kyoto, Japan (NTIS Access No. PB-298-025).*

CCIR (1978i), Report 558-1, Satellite antenna patterns in the fixed satellite service, Vol. IV, Fixed Service Using Communication Satellites, CCIR XIV Plenary Assembly, Kyoto, Japan (NTIS Access No. PB-298-024).*

* National Technical Information Service (NTIS), 5285 Port Royal Road, Springfield, VA 22161.

CCIR (1978j), Report 391-3, Radiation diagrams of antenna for earth stations for the fixed satellite service for use in interference studies and for the determination of design objective, Vol. IV, Fixed Services Using Communication Satellites, CCIR XIV Plenary Assembly, Kyoto, Japan (NTIS Access No. PB-298-024).*

CCIR (1978k), Report 724, Propagation data for the evaluation of coordination distance in the frequency range 1 to 40 GHz, Vol. V, Propagation Through Non-Ionized Media, CCIR XIV Plenary Assembly, Kyoto, Japan (NTIS Access No. PB-298-025).*

CCIR (1978 l), P/58-E, Depolarization by Ice Particles on Earth-Space Paths, U. K. Input Document to the special Preparatory Meeting (SPM), 29 May 1978, Geneva.**

CCIR (1978m), Annex I of Report 814, Factors to be considered in the choice of polarization for planning the broadcasting-satellite service, Vol. XI, Broadcasting Service (Television), CCIR XIV Plenary Assembly, Kyoto, Japan (NTIS Access No. 298-031)*.

Crane, R. K. (1976), Low elevation angle measurement limitations imposed by the troposphere, an analysis of scintillation observations made at Haystack and Milstone, MIT Lincoln Lab Tech. Rept. 518, Lexington, Mass.

Crane, R. K. (1978), Analysis of tropospheric effects at low elevation angles, RADC-TR-78-252, RADC/EEP, Hanscom AFB, MA.

Crane, R. K. (1980), Prediction of attenuation by rain, Trans, IEEE COM 28, (accepted for publication).

Dougherty, H. T. (1968), A survey of microwave fading mechanisms, remedies, and applications (NTIS access No. COM-71-50288).*

Dougherty, H. T., and E. J. Dutton (1978), Estimating year-to-year variability of rainfall for microwave applications, IEEE Trans. Commun. COM-26, No. 8, 1321-1324, August.

Dougherty, H. T. and B. A. Hart (1979), Recent progress in duct propagation predictions, IEEE Trans. AP-27, No. 4, 542-548, July.

Dougherty, H. T. (1980), On polarization orientations for satellite systems, NTIA Report 80- (in preparation).

Dutton, E. J. (1977), Earth-space attenuation prediction procedures at 4 to 16 GHz, OT Report 77-123 (NTIS Access No. PB-269-228).*

Dutton, E. J., and H. T. Dougherty (1978), Estimates of the atmospheric transfer function at SHF and EHF, NTIA Report 78-8 (NTIS Access No. PB-286-632), August.*

Dutton, E. J., and H. T. Dougherty (1979), Year-to-year variability of rainfall for microwave applications in the U.S.A., IEEE Trans. Commun. COM-27, No. 5, 829-832, May.

EEH (1975), Electronics Engineers' Handbook, D. G. Fink, Editor, McGraw-Hill, N.Y.

---

* National Technical Information Service (NTIS), 5285 Port Royal Road, Springfield, VA 22161.

GSFC (1974), The ATS-f Data Book, NASA's Goddard Space Flight Center Technical Report 1418, December.

GSFC (1978), Prediction of Millimeter Wave Propagation Effects on Earth-Space Paths, NASA's Goddard Space Flight Center Technical report 1418, December.

ITT (1969), Reference Data for Radio Engineers, Fifth Edition (H. W. Sams & Co., Inc., N.Y.)

ITU (1976a), Radio regulations, Article 7, Spa 2, Section VIII, Space radio-communication services sharing frequency bands above 1 GHz, §21 power limits, Earth Stations Footnotes 470 G, ITU, Geneva.**

ITU (1976b), Radio regulations, Article 7, Spa 2, Section VIII, Space radio-communication services sharing frequency bands above 1 GHz, §23, Limits of Power Flux Density from Space Stations, Footnotes 470 N through 470 NZA, ITU, Geneva.**

ITU (1979), Chapter 2, Section 5, Earth-Space Systems of the Manual on Local Network Planning (GAS 2, 1979 Edition), International Telecommunication Union, General Secretariat-Sales Section.**

Morgan, W. L. and C. D. Gordon (1976), Satellite Service Calculator, COMSAT Labs, Clarksburg, MD 20734.

Morgan, W. L. (1979), Ever smaller earth stations, crowded satellites imply changes, Microwave Systems News 9, No. 4, April, 8190.

Rice, P. L., A. G. Longley, K. A. Norton, and A. P. Barsis (1966), Transmission loss predictions for tropospheric communication circuits, Vol. I, NBS Tech. Note No. 101 (NTIS Access No. AD 687820).*

Shkarofsky, I. P. and H. J. Moody (1976), Performance characteristics of antennas for direct broadcasting satellite systems including effects of rain depolarization, RCA Review 37, 49-50, September.

Skolnik, M. I. (1970), Radar Handbook (McGraw-Hill, NY).

Yeh, L. P. (1972), Geostationary satellite orbital geometry, IEEE Trans. Commun. Com-20, No. 2, April, 252.

APPENDIX A
SATELLITE/EARTH-STATION GEOMETRY

For an earth-space system, the space terminal or satellite will move around the earth in an orbit that may be approximated by the two-body solution as an ellipse. The ellipse will have one of its foci at the earth's center, as shown in Figure A1, and the radial distance, ρ in kilometers, from the earth's center to the satellite is given by

$$\rho(\psi) = \frac{a(1 - e^2)}{1 + e \cos \psi} . \tag{A1}$$

Here:

ψ is the directional angle measured in the orbiting plane relative to the direction to the perigee (point of minimum ρ) at P;

e   is the ellipse's eccentricity, $0 \le e < 1.0$. which is zero for a circular orbit; and

a   is the semi-major axis in kilometers.

The value of a in kilometers may be determined for the orbital period, T in hours, from

$$a = \nu \, T^{2/3}, \ \nu = \left[\frac{\mu}{4\pi^2}\right]^{1/3} . \tag{A2}$$

Here, the μ is the product of the gravitational constant and the mass of the earth, $\mu \simeq 5.1658 \, (10)^{12} \ km^3/h^2$. Therefore, $\nu = 5076.8 \ km/h^{2/3}$. An orbiting satellite has a constant angular momentum per unit mass of the satellite; this may be determined as a product of the tangential velocity at perigee, v_t ($\psi = 0°$) in kilometers per hour, and the radial $\rho(\psi = 0°)$ in kilometers. The ellipse eccentricity is then

$$e = \left[1 - \frac{\rho^2(\psi = 0°) \, v_t^2(\psi = 0°)}{\mu a}\right]^{1/2} . \tag{A3}$$

At perigee, the elevation of the satellite is $\rho(\psi = 0°)$ less the earth radius of 6378 km. The constant total energy (kinetic plus potential) of an orbiting satellite mass, m in kilograms, is given by

$$W = \frac{\mu m}{2a} \ kg \ k_m^2 \ /h^2 . \tag{A4}$$
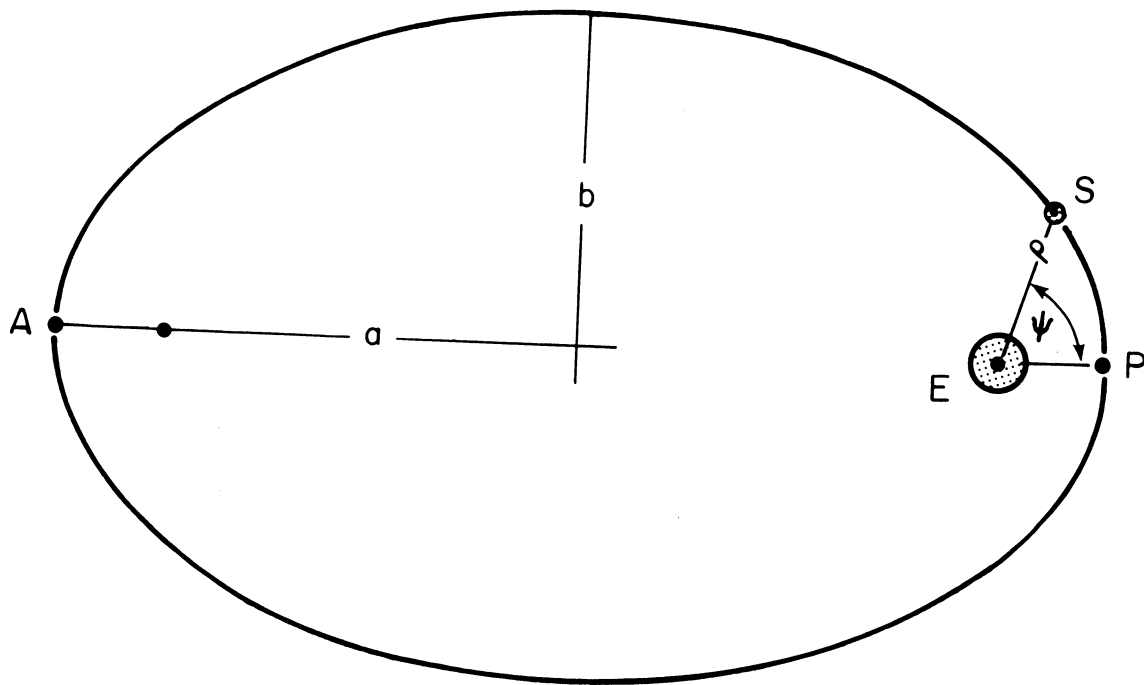
Figure A1. Elliptical orbit about the earth. The semi-major axis is a.
For the perigee at P, ρ ($\psi = 0°$) is a(1 - e); for the apogee
at A, ρ ($\psi = 180°$) is a(1 + e). The semi-minor axis is
b = a(1 - e^2)$^{1/2}$. The eccentricity is e = [1 - b^2a^2]$^{1/2}$.

Dividing the result of (A4) by 12.96 will express the energy in joules. At perigee $\rho(\psi = 0°) = a(1 - e)$; at apogee, $\rho(\psi = 180°) = a(1 + e)$. The instantaneous velocity of the satellite is

$$v = \mu^{1/2} \left[\frac{2}{\rho} - \frac{1}{a} \right]^{1/2} \text{ km/h .} \tag{A5}$$

Of course, the fixed earth terminal has a velocity $v = (R_0 \pi/12) \cos L$ km/h, where L is the earth terminal's latitude and R_0 is the earth's radius (R_0 = 6378 km).

Note that for a period of T = 24 hours, (A2) yields a value of

$$a = 5076.8(24)^{2/3} = 42{,}241 \text{ km}$$
$$= 6378 + 35{,}863$$

or a geosynchronous altitude ($\psi = 0$, $\rho = a$) of 35,864 km. However, an earth-orbiting satellite does not constitute a simple two-body problem assumed for (A1) through (A5). NASA has determined the synchronous altitude to be approximately 35,785 km above an earth of radius R_0 = 6378; i.e., $\rho(\psi = o)$ = 42,163 km [GSFC, 1974].

The geometry of a geosynchronous satellite S, its subsatellite point SS, and its earth station ES, are illustrated in Figure A2. The four parameters:

Z, the angular distance in degrees (Z°) or the great-circle arc in kilometers (Z_{km} = 111.32 Z°) from ES to SS;

ε, the elevation angle in degrees above the horizontal from ES toward S);

φ, the angle of arrival in degrees relative to the radial at S;

and

r, the range in kilometers from ES to S

are directly related. Given one, the other three are readily determined from

$$\sin \phi = \frac{R_0 \cos \epsilon}{R_0 + H} = \frac{R_0 \sin Z°}{r} \tag{A6a,b}$$

$$r^2 = R_0^2 + (R_0 + H)^2 - 2R_0(R_0 + H) \cos Z° \tag{A6c}$$

$$\phi + \epsilon + Z° = 90° \tag{A6d}$$

where the earth radius R_0 is 6378 km and H is the satellite elevation, or minimum earth-satellite range of 35,785 km. These relationships are plotted in Figure 1 of the text.
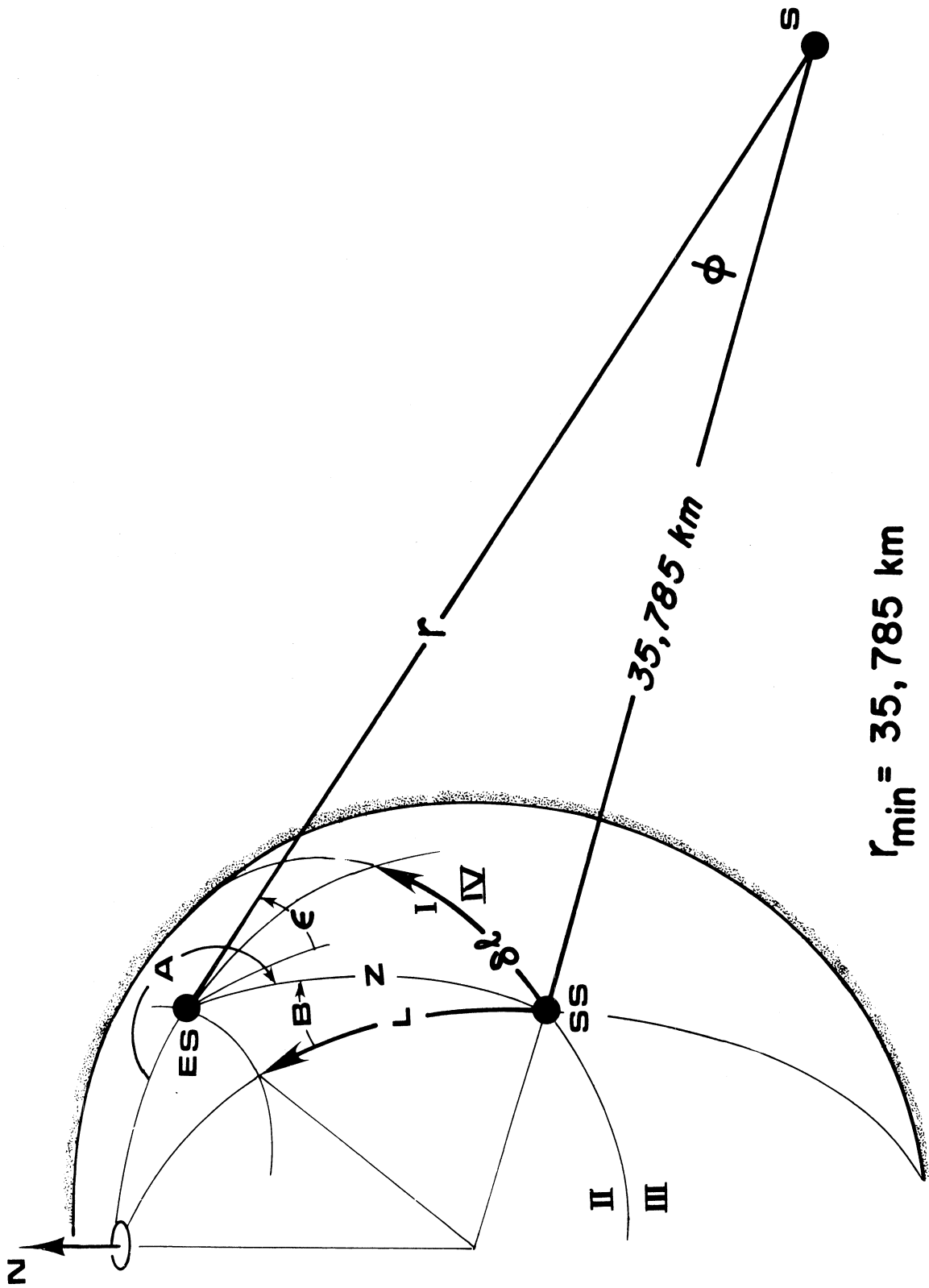
Figure A2. Synchronous satellite geometry.

$r_{min} = 35,785$ km

67

The location of the earth station relative to the subsatellite point is given by any two of the five parameters:

L   the latitude of ES in degrees;

δℓ   the longitude of ES east of SS in degrees;

A   the azimuth in degrees from ES to SS;

B   the back azimuth in degrees from SS to ES;

and

Z   the great circle arc.

These are related by

$$\cos Z° = \tan B/\tan (A-180) = \cos L \cos \delta\ell$$
$$\cos (A-180) = \tan L/\tan Z = \cos \delta\ell \cos B$$
$$\sin L = \tan \delta\ell/\tan (A-180) = \sin Z \cos B \tag{A7}$$
$$\sin \delta\ell = \tan L (\tan B) = \sin Z \sin (A-180)$$
$$\sin B = \tan \delta\ell/\tan Z = \cos L \sin (A-180) \ .$$

The relationship between L, δℓ, B, and Z are plotted in Figure A3. A similar plot for L, δℓ, A, and Z are shown in Figure 3 of the text. Both figures give the azimuths for positive (Quadrant I) values of L and δℓ. The following Table A1 lists the corresponding values of   B for other values of L and δℓ, as in the Quadrants II, III, and IV identified in Figure A2.
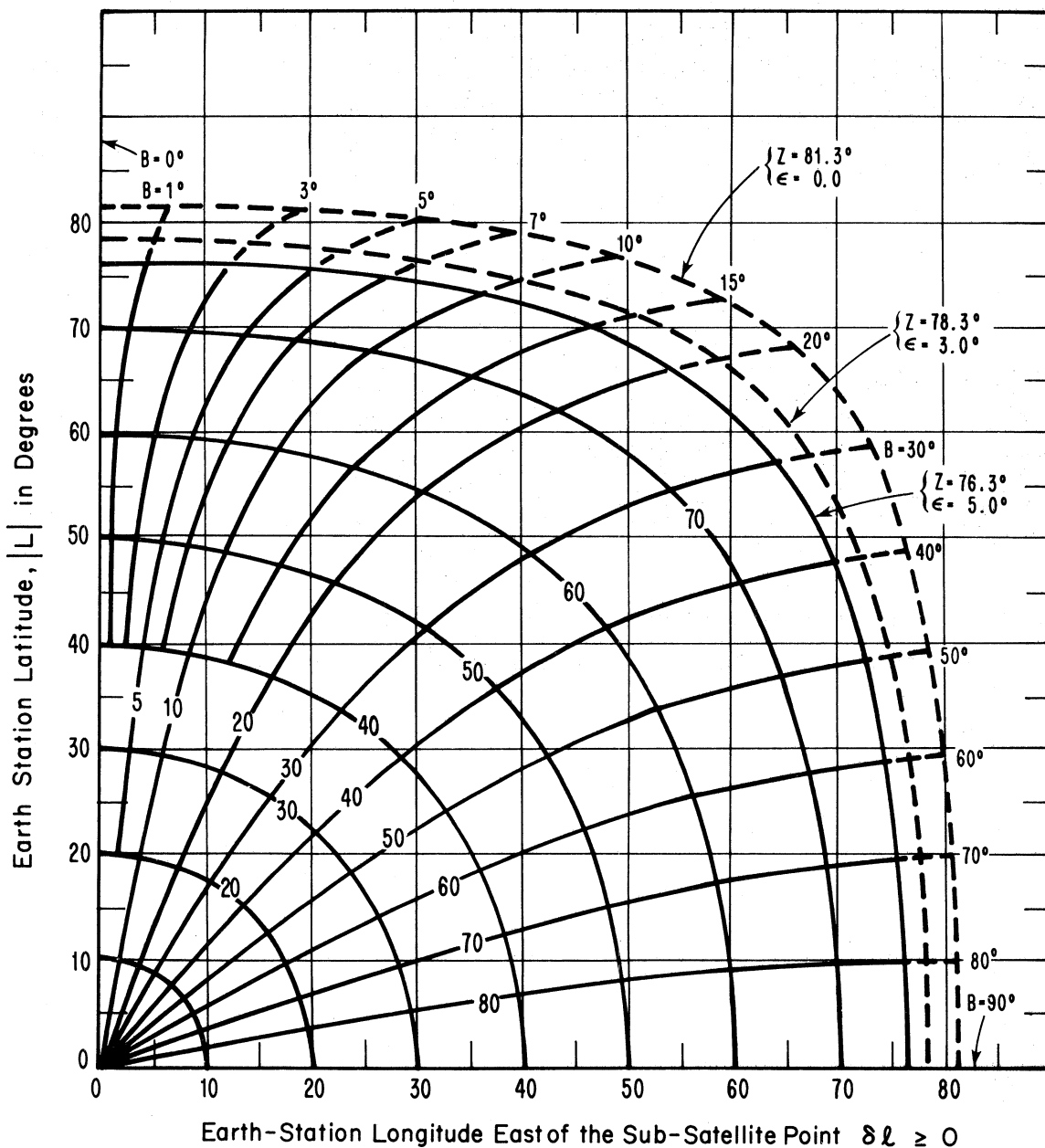
Figure A3. The great-circle arc (Z) and the back-azimuth (B, from SS to ES) as a function of the earth-station's (ES) north latitude L and degrees of longitude (δℓ) east of the sub-satellite point (SS).

Table A1

Tabulation of Back-Azimuths, B from SS to ES[†], as a Function
of ES Latitude, L, and Relative Longitude, $\delta\ell$*

$\delta\ell < 0$		$\delta\ell > 0$	
L ≤ 0	L ≥ 0	L ≥ 0	L ≤ 0
B = 270°	B = 270°	B = 90°	B = 90°
260	280	80	100
250	290	70	110
240	300	60	120
230	310	50	130
220	320	40	140
210	330	30	150
200	340	20	160
190	350	10	170
100	360	0	180
QIII	QII	QI	QIV

[†] ES is earth-station location, SS is subsatellite point.

* degrees of longitude that ES lies <u>east</u> of SS.

APPENDIX B
Depolarization due to Disparate Definitions

In the case of linear polarization, the definition of horizontal and vertical polarization is largely a matter of convention. For terrestrial telecommunication links, the convention is based on the definition of a propagation plane containing the great-circle propagation path between two terminals and therefore both earth radii through the path terminals. A vertically polarized radiated EM wave is then one having its electric field vector lying in this propagation plane and normal to the direction of the wave trajectory (for far-field effects of properly directed antennas). A horizontally polarized wave has its electric field vector normal to the propagation plane. See the discussion on reflection in any electromagnetic theory text.

Strictly speaking, since the propagation plane is defined by the geometry of each terrestrial link, this defines vertical and horizontal polarization uniquely for each telecommunication link. Until recently, there was little need to stress this uniqueness of definition. For example, for terrestrial systems, the direction of vertical polarization is adequately approximated as the local vertical (radial) direction and the direction of horizontal polarization is adequately approximated as normal to the azimuthal direction of propagation and to the local radial.

For earth/space systems, these approximations are seriously misleading. Consider the application of the definitions to the telecommunication link (S_1/ES_1) in Figure B1. This link would have parallel vertical polarization unit vectors, $\overline{V_1}$, at an angle $0° \leq \varepsilon \leq 90°$ from the earth-station's localized radial at ES_1 and at angle $81° < 90 - \phi \leq 90°$ from the satellite's local radial at S_1. The direction of the horizontal polarization unit vectors, $\overline{H_1}$, are also parallel and normal to the plane through the earth's center 0 and the terminals at S_1 and ES_1. Note, however, that looking from another earth station ES_2 (on the equator) toward S_1, the S_1 vertical polarization unit vector appears to be "depolarized" by an angle $80° < 90 - \phi \leq 90°$ and within $10°$ of the horizontally polarized unit vector $\overline{H_2}$.

This "depolarization" results from the necessarily disparate definitions and is assessable from the two-system geometry of Figure B2 from the parameters:

B_1 the back azimuth from subsatellite point SS_1 to the earth-station S_1

Z_1 and Z_i the great-circle arcs from SS_1 to the earth-stations, respectively, to ES_1 and ES_2
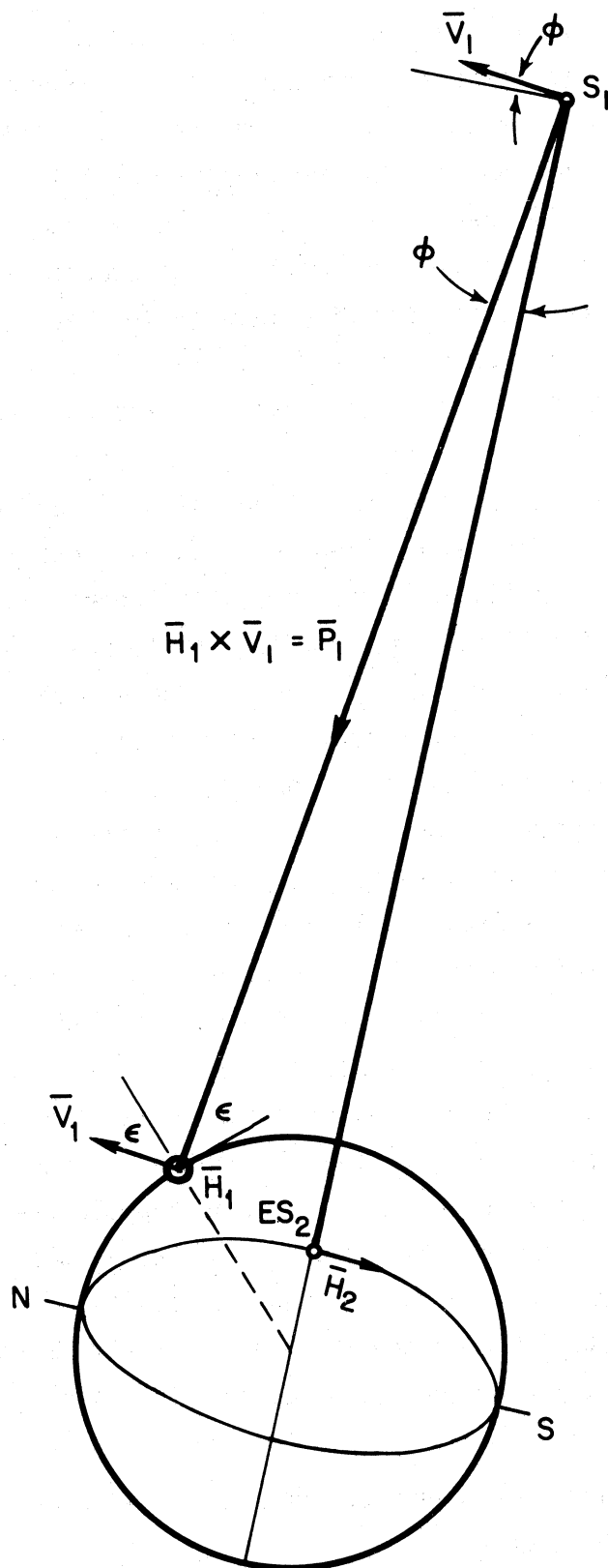
Figure B1. Polarization geometry. The polarization vectors $\overline{H}_1$ and $\overline{V}_1$, are for the path of elevation angle ε, the polarization vector $\overline{H}_2$ is for the path ES_2/S_1. H_1 is normal to the page.
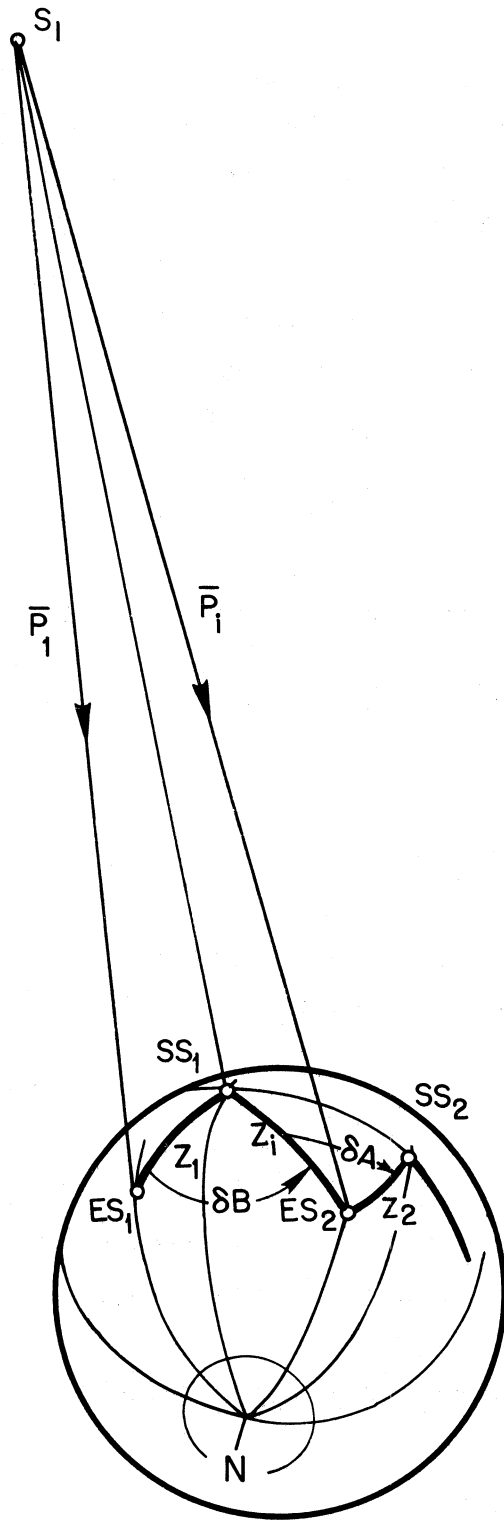
Figure B2. Potential interference geometry. $\overline{P}_1$ is a propagation vector for the service path ES_1/S_1 and $\overline{P}_i$ is the propagation vector for the potential interference path S_1/ES_2.

δB the difference in back azimuths $\delta B = B_1 - B_i$

δA the difference in azimuths $\delta A = A_2 - A_i$

$\delta \ell_i$ the difference in longitude between the subsatellite points S_1 and SS_2.

These permit the determination of the geometrical parameters A, B, ϕ, and ε from the great-circle arc for the satellite/earth-station paths (ES_1/S_1, ES_2/S_2, and ES_2/S_2) with associated subscripts 1, i, and 2 by means of the relationships of Appendix A. These permit determination of the directional cosines

$$C_{VS} = \sin\phi_1 \sin \phi_i + \cos \phi_1 \cos \phi_i \cos \delta B, \tag{B1}$$

$$C_{VES} = \cos \varepsilon_2 \cos \varepsilon_i + \sin \varepsilon_2 \sin \varepsilon_i \cos \delta A, \tag{B2}$$

$$C_{HS} = \cos \delta B, \qquad C_{HES} = \cos \delta A, \tag{B3,4}$$

$$S_{1S} = \cos \phi_1 \sin \delta B, \qquad S_{iS} = \cos \phi_i \sin \delta B, \tag{B5,6}$$

$$S_{2ES} = \sin \varepsilon_1 \sin \delta A, \qquad S_{iES} = \cos \varepsilon_i \sin \delta A. \tag{B7,8}$$

From these we may determine the rotational coefficients

$$C_a = C_{HES}C_{HS} + S_{iES}S_{iS} \tag{B9}$$

$$-C_b = S_{iES}C_{VS} - S_{1S}C_{HES} \tag{B10}$$

$$C_c = C_{VES}S_{iS} - S_{2ES}C_{HS} \tag{B11}$$

$$C_d = C_{VES}C_{VS} + S_{2ES}S_{1S} . \tag{B12}$$

For isotropic transmitting and receiving antennas, the orientation of the received interference field at ES_2 due to a source on S_1 is (in the absence of any atmosphere) given by

$$\overline{E} = \overline{H_2} \left[CC_a - SC_b \right] + \overline{V_2} \left[CC_c + SC_d \right]. \tag{B13}$$

The coefficients $C = \cos \beta$ and $S = \sin \beta$ are used to separate the effects of linear polarization. For only a vertically polarized source, $\beta = 90°$. For only a horizontally polarized source, $\beta = 0°$.

The geometrical depolarization angle is given by

$$\theta_H = \text{arc tan} (C_c/C_a) , \tag{B14a}$$

74

for a horizontally polarized signal transmitted from satellite S_1 that is received as interference by an earth-station ES_2 whose antenna is directed for reception of (desired) signals from S_2. Similarly, the geometrical depolarization for a vertically polarized transmitting signal is given by

$$\theta_V = \text{arc tan } (C_d/C_b) \ . \tag{B14b}$$

The rotational angle, $\theta_0 = \theta_H$ or θ_V, are illustrated in Figure 15 of the text, and

$$\theta_0 = \delta B - \alpha \delta A, \tag{B15}$$

generally to within a few degrees, usually within a degree. The coefficient α is a function of Z_i, δB, and δA, given by Figure 16 of the text.

For the situation where the interference path between S_1 and ES_2 is for the source at ES_2, and the satellite S_1 is the victim, the previous expressions hold with a minor change. That change is to interchange, in (B13) and (B14a), the $-C_b$ and C_c.

For the interference path between S_2 and ES_1, the foregoing expressions will hold if the subscripts 1 and 2 are interchanged in the expressions (B1) through (B12). The great-circle arc Z_i is then between ES_1 and SS_2 in Figure B2.

A detailed derivation of the foregoing is planned by the author [Dougherty, 1980].

Appendix C
Depolarization for Circular Polarization

Consider the effect of depolarization upon a transmitted, initially-circularly-polarized signal. That transmitted signal may be represented as the right-hand circularly polarized signal

$$\overline{E}_t = A \left[\cos \upsilon \, \overline{u}_H + \sin \upsilon \, \overline{u}_V \right] , \tag{C1}$$

represented as the sum of two orthogonal, linearly-polarized equal-amplitude signals in phase quadrature. As a result of depolarization (either the unequal attenuation and phase-shift differentials of atmospheric depolarization by rainfall, ice crystals, etc., or the geometrical depolarization of disparate definitions), the signal will be received as an elliptically polarized signal. An elliptically polarized signal is representable as either

$$\overline{E}_r = r_1 \cos \upsilon' \, \overline{u}_H + r_2 \cos (\upsilon' - \Phi) \, \overline{u}_V \tag{C2a}$$

or

$$\overline{E}_r = a \cos \upsilon'' \, \overline{u}_H + b \sin \upsilon'' \, \overline{u}_V . \tag{C2b}$$

However, it is also representable as the sum of two circularly polarized signals, one right-hand circular and one left-hand circular

$$\overline{E}_r = \overline{E}_{RHC} + \overline{E}_{LHC}$$

$$= \frac{a + b}{2} \left[\cos \upsilon''' \, \overline{u}_H + \sin \upsilon''' \, \overline{u}_V \right] \tag{C3}$$

$$+ \frac{a - b}{2} \left[\cos \upsilon''' \, \overline{u}_H - \sin \upsilon''' \, \overline{u}_V \right] .$$

Here

$$a \pm b = \sqrt{r_1^2 + r_2^2 \pm 2 r_1 r_2 \sin \Phi} . \tag{C4}$$

The elliptical ratio would be

$$b/a = \tan \left[1/2 \arcsin (\sin 2 \mu \sin \Phi) \right] \tag{C5}$$

with the major axis tilted at an angle given by

$$\frac{1}{2} \arctan\left[\tan 2\mu \cos \Phi\right], \tag{C6}$$

where $\mu = \arctan (r_2/r_1)$. $\tag{C7}$

Application to Geometrical Depolarization

In the case of geometrical depolarization by disparate definitions, from Appendix B we can write

$$\overline{E}_r = E_o \{[CC_a - SC_b] \overline{u}_H + [CC_c + SC_d] \overline{u}_V \} \quad, \tag{C8}$$

in the absence of an atmosphere and other sources of depolarization, for the notation $C = \cos \theta$, $S = \sin \theta$, and for isotropic antennas. If we use the relationship

$$a_j \cos \theta' + b_j \sin \theta' = r'_j \cos (\theta' - \Phi_j) \tag{C9a}$$

where

$$r'_j = \sqrt{a_j^2 + b_j^2} \quad, \quad \Phi_j = \arctan (b_j/a_j) \tag{C9b,c}$$

to write (C8) in the form of (C2a). Then,

$$r'_1 = \sqrt{C_a^2 + C_b^2} \quad, \quad \Phi_1 = \arctan (C_b/C_a) \tag{C10a}$$

$$r'_2 = \sqrt{C_c^2 + C_d^2} \quad, \quad \Phi_2 = \arctan (C_d/C_c) \tag{C10b}$$

and

$$\Phi = \Phi_2 - \Phi_1 \quad. \tag{C10c}$$

The primes on the r'_1 and r'_2 are to distinguish them from the required r_1 and r_2 of (C4). Since the field is propagated as an <u>electromagnetic</u> wave $\overline{P} = \overline{E} \times \overline{H}$, the significant field amplitudes are the projections of $\overline{E}$ and $\overline{H}$ upon the plane normal to the direction $\overline{P}$ of propagation and in the ratio $E'/H' = 120 \pi$, the impedance of free-space. For example, for a horizontally polarized wave, the magnitude of the projected electric field vector is r'_1 ; the projected magnetic field vector is r'_2. However, the required equivalency of their ratio to 120π means that the propagated field strength $\hat{r}$ is the lesser of r'_1 and r'_2 . Further,

$$\Phi = 90 - \Delta\theta_o, \tag{C11}$$

77

where $\Delta\Theta_o$ is the difference in rotation of the horizontal and vertical fields (because of disparate definitions). Therefore, from (C3) and (C4)

$$E_{RHC} = \hat{r} \cos \frac{\Delta\Theta_o}{2} \quad , \quad E_{LHC} = \hat{r} \sin \frac{\Delta\Theta_o}{2} \qquad \text{(C12 a,b)}$$

and

$$XPD_C = -20 \log \tan \frac{\Delta\theta_o}{2} \quad . \qquad \text{(C12c)}$$

For the depolarization of the circularly polarized wave due to disparate definitions, $\Delta\theta_o \leq 1°$ and $XPD_C > 40$ dB.

A somewhat more detailed derivation of the foregoing is planned by the author [Dougherty, 1980].

Appendix D
Atmospheric Refraction at Low Angles

For elevation angles of $\varepsilon \leq 5°$, the earth-station/synchronous-satellite propagation-path parameters become increasingly sensitive to tropospheric stratification, specifically refractivity layering. For example, in Figure 3 of the text, the dashed curves for $Z < 76.33°$ ($\simeq 8497$ km), $\varepsilon < 5°$ are those appropriate in the absence of an atmosphere. To determine the average atmospheric effects, we note that for radio propagation purposes, the long-term median atmosphere may be approximated by an exponential refractivity structure with a surface value N_s [Bean and Thayer, 1959]. Figure 5 of the text illustrates a comparison of observations and predictions; the $\overline{\varepsilon - \varepsilon_0}$ values were observed for $N_s \simeq 332$ with $\varepsilon_0 \leq 40$ and for $N_s \simeq 358$ with ε_0 at about 60 to 65°.

Table D1 is a tabulation of N_s seasonal values $200 < N_s < 450$ that can be observed across the U.S.A. [Bean et al., 1960]. The corresponding Z values (from the SS point to the satellite's horizon) are tabulated. Note, that for $N_s = 0.0$ or free-space conditions, the distance to the satellite's horizon is $Z_0 \simeq 81.3°$ or 8497 km. For the tabulated N_s values we see that the corresponding Z values increase with N_s value and the radio horizon can be extended appreciably, by δZ beyond the free-space value.

Of course, the actual refractivity structure commonly departs markedly from the median exponential structure, both near the surface and aloft (but within a kilometer or so of the surface) so that the median structure can be misleading. These departures from the median structure take the form of refractivity layers with strong refractivity gradients whose effects at low elevation angles can readily provide a great-circle just-barely-line-of-sight distance that is either shorter than that indicated in Figure 3 or much longer than those computed in Table D1 for the median atmosphere [Dougherty, 1968; Dougherty and Hart, 1979]. In fact, by ducting (the trapping of radio waves by super-refractive layers), an earth station for which $Z > 76°$ could be effectively isolated from the corresponding satellite. The remedies for these severe refraction effects are to either observe a design criterion such as $\varepsilon \geq 5°$ or employ adaptive techniques.

TABLE D1

Median Extension of Horizon for a Median Exponential Atmosphere

N_S	Z (in degrees)	δZ (in kilometers)
0.0	81.2994	0.0
200.0	81.7119	45.9
252.9	81.8493	61.2
289.0	81.9643	74.0
313.0	82.0587	84.5
344.5	82.2037	100.7
377.2	82.3921	121.6
404.9	82.5919	143.9
450.0	83.0836	198.6

Appendix E
List of Symbols in Text*

a	is the field attenuation ratio, (18a).
A	is the azimuth from ES to SS in degrees, Figs. 2, 3, Table 1.
A( )	is the atmospheric attenuation expressed in decibels and as an explicit function of the parameters (p,ε, etc.) whose symbols are contained within the parentheses; (11), (12), Figs. 7, 8.
A_i( )	is the atmospheric attenuation in decibels subscripted with an "i" to indicate association with the interference path, (28).
A( )	is the atmospheric attenuation expected to be exceeded for less than the single-site probability (p_1 in the parentheses) or the joint probability (p_2 in the parentheses), (17), Fig. 9.
B	is the back-azimuth from SS to ES in degrees, (3b), Fig. A3, Table A1.
Bw	is the system noise bandwidth in Hertz, (9), (10), (19).
Bw´	is a reference system bandwidth in Hertz, (20a), (20b), Table 4.
c	is a corrective factor for a non-uniform distribution of signal power over a system bandwidth, (20b); C = 10 log c.
CPA	is the received co-polarized signal attenuation in decibels, CPA = 20 log a, (15c), (18b), (37a).
C	is the cosine of an angle.
$(c/i)_{dB}$	is the signal carrier-to-interference ratio in decibels, (29).
$(c/n)_{dB}$	is the signal carrier-to-noise ratio in decibels, (26).
$(c/T)_{dB}$	is the earth-space figure of merit in decibels, (23).
d	is the ES/SS interference path length in kilometers, (29).
D	is the parabolic-dish-antenna diameter in meters, (34a), (34b), (34c), Table 2.
ES	is the earth-station location, Figs. 1, 2, subscripted to identify a particular system.
f	is the transmission frequency in gigahertz, (1), (2).
f_R	is the receiving system noise figure, (10).
g	is the antenna power gain relative to that of isotropic antenna. It is primed to indicate the gain is exclusive of line and radome losses. It is subscripted to indicate its association with an earth-station (ES) or satellite (S) or with a transmitting (T) or receiving (R) terminal, Table 2.

---

* Equation, Figure, or Table numbers identify where the symbols first appear and/or are defined.

G	is the antenna power gain expressed in decibels above an isotropic antenna. The omission of a prime indicates that the value of antenna gain in decibels has been reduced by inclusion of line and radome losses, (34b), Table 2. It is subscripted to indicate association with an earth-station (ES), satellite (S), transmitting terminal (T), or receiving terminal (R).
G'_o	is the main-beam antenna gain in decibels above an isotropic antenna's gain, (32a), (34b), Figs. 10, 11.
$G'(\ )$	is the off-axis antenna gain in decibels above an isotropic antenna as an explicit function of the off-axis angle Δ or its ratio to the half-beamwidth angle, Δ/Δ_o, (32a), (33a), Figs. 10, 11. It may be subscripted to indicate association with an earth-station or satellite.
H	is the elevation of an earth-station or radio terminal in meters above mean-sea-level (MSL), (11).
i	is the subscript appended to the interference system parameter, (28), (29), Fig. 14. It can also represent a numerical subscript, as in Section 5.2.
I_R	is the undesired-signal (interference) received power in decibels above one watt, (28), (29).
j	is a numerical subscript to identify a particular system's parameter, as in Section 5.2.
k	is the Boltzman constant, (7), (8). It is also a numerical subscript in Section 5.2.
L	is the degrees of latitude, positive for North Latitude and negative for South Latitude, Figs. 2 and 3, Table 1.
L	is the system transmission loss in decibels.
L_o	is the free-space transmission loss in decibels, (1).
L_{bo}	is the free-space basic transmission loss in decibels, (1).
m	is the exponent in defining a portion of the satellite antenna reference pattern, (32b).
n	is the parameter used in defining a portion of the earth-station dish-antenna reference pattern in terms of the diameter-wavelength ratio, (33b).
n	is the receiving system total noise power in watts, (9), (10).
n_e	is the external noise-power spectral density in watts/hertz, (7), (18).
N_e	is the external noise-power spectral density in decibels above one watt/hertz, (8).
$N(p)$	is the total system noise power, in decibels above one watt per hertz, exceeded for p percent of all hours of a year, (17c).
p	is the power in watts, subscripted by T for transmitted power and by R for received power, (1).
p_1/p_2	is the diversity advantage for site-diversity, the ratio of the single-site probability to the joint probability for the common attenuation value, Fig. 9.

P	is the power in decibels above one watt, subscripted by T or R for, respectively, transmitted or received power, (1).
$P_R(p)$	is the received signal power value, in decibels above one watt, expected to be exceeded for all but p percent of all hours of a year, (17d).
PFD	is the power flux density in watts per hertz of specified bandwidth, (20a), (20b), Table 4.
Q	is the parameter used in defining the earth-station dish-antenna reference pattern (35b).
r	is the subscript appended to various parameters to indicate the value expected in the presence of rainfall, (37a), (37b).
r	is the propagation path length or range, in kilometers, between an earth-station and a satellite, (2), (27), Figs. 1, 2.
R	is the subscript for parameters associated with a receiving terminal (1), (2).
R_0	is the earth's radius in kilometers, here taken to be 6378 km, Figs. 1, 2.
s	is the exponent in defining a portion of the earth-station dish-antenna reference pattern, (33b).
S	is the antenna aperture area in square meters, Table 2.
S	is the geosynchronous satellite position, subscripted for association with a particular system, Figs. 1, 2.
SS	is the sub-satellite position on the equator, subscripted for association with a particular statellite, Figs. 2, 14.
$S(\varepsilon - \varepsilon_0)$	is the observed standard deviation of the elevation angle's scintillation or departure from its geometrical or equivalent free-space value, Fig. 5.
$S'(\varepsilon - \varepsilon_0)$	is the expected total standard deviation of the elevation angle's scintillation due to both tropospheric and ionospheric effects, (6).
$T_e(\ )$	is the external noise temperature in degrees Kelvin, OR in decibels above a reference temperature (290°K), Fig. 6.
T_R	is the receiver noise temperature in degrees Kelvin, (9), (10).
T	is the total system equivalent receiver noise temperature in degrees Kelvin, (10), (21).
$T(p,\varepsilon)$	is the total system equivalent receiver noise temperature value expected to be exceeded for p percent of all hours at an elevation angle of ε degrees.
W	is the power flux density expected at the earth's surface for radio wave transmission from a satellite in decibels above one watt per square meter, (18a), (18b).
x	is the expected cross-polarized received signal stength, (37b), Fig. 17.
XPD	is the cross-polarized received signal strength in decibels below the transmitted signal, (38a), Fig. 17.

y	is the expected co-polarized received signal strength, (37a), Fig. 17.
Z	is the great-circle arc between ES and SS expressed in degrees (of central angle) or kilometers, (Figs. 1, 2, 3.
α	is the proportionality factor in determining geometrical depolarization, (36), Fig. 15.
δ	is the loss factor due to signal depolarization and polarization discrepancy between transmitting and receiving antennas, $\delta = \cos\theta$.
δ_o	is the free-space loss factor due to depolarization discrepancy between transmitting and receiving antennas, $\delta_o = \cos\theta_o$, (2).
δA	is the difference in azimuths in degrees, $\delta A = A_1 - A_2$ or $A - A_i$, (31b).
δB	is the difference in back-azimuths in degrees, (3b), $\delta B = B - B_i$.
$\delta \ell$	is the earth-station longitude measured in degrees east of the sub-satellite point. It is taken as negative if measured west of the sub-satellite point.
δZ	is the difference in great-circle arc lengths, (3a).
$\delta A(p)$	is the signal margin provided by site diversity, (17).
Δ	is the off-axis direction angle measured in degrees from the mainbeam antenna orientation and the direction of interest. Subscripts are appended to indicate association with a particular terminal (ES or S) or a particular value of the reference antenna pattern (Δ_1 or Δ_2), (30), (31a).
Δ_o	is the off-axis directional angle in degrees corresponding to the mainlobe half-power point or one-half of the mainlobe beamwidth, (32c), (34c).
Δ/Δ_o	is the off-axis directional angle normalized to the mainlobe half-beamwidth, (32a), Figs. 10, 11. Subscripts, 1 or 2, identify specific values (Δ/Δ_o), etc., (35b).
ΔG	is the off-axis reduction in gain in decibels due to the antenna pattern. Subscripts, ES or S, identify the associated pattern, (32a), (35a), Figs. 10, 11.
ε	is the earth-station's elevation angle in degrees for the propagation path to a geosynchronous satellite, Figs. 1, 2, 3.
ε_o	is the earth-station's elevation angle that would apply in the absence of an atmosphere or for simple straight-line earth-station/satellite geometry, Fig. 5.
$\overline{\varepsilon - \varepsilon_o}$	is the mean departure of the observation elevation angle from its equivalent free-space value.
η	is the antenna efficiency, (5), Table 2.
θ_o	is the depolarization angle (discrepancy between earth-station and satellite polarization orientations) due to geometry and the disparity in definition, (36), (40), Fig. 15.
θ_i	is the depolarization of a slant-path signal expected due to Faraday rotation in the ionosphere, (13), (40).
θ_r	is the depolarization of a slant-path signal expected due to rainfall, (39), (40).

λ is the radio wave transmission wavelength in meters, (34a), Table 2.

ϕ is the acute angle measured in degrees from the vertical (radially) at a synchronous satellite, Fig. 1, 2.

Ω is the antenna beamwidth in degrees, (32c).

BIBLIOGRAPHIC DATA SHEET

	1. PUBLICATION OR REPORT NO. NTIA Report 80-45	2. Gov't Accession No.	3. Recipient's Accession No.

4. TITLE AND SUBTITLE
A consolidated model for UHF/SHF telecommunication links between earth and synchronous satellites

5. Publication Date
August 1980

6. Performing Organization Code
NTIA/ITS3

7. AUTHOR(S)
H. T. Dougherty

9. Project/Task/Work Unit No.

8. PERFORMING ORGANIZATION NAME AND ADDRESS
U. S. Dept of Commerce
NTIA/ITS3, 3413-1
325 Broadway
Boulder, CO 80303

10. Contract/Grant No.

11. Sponsoring Organization Name and Address

12. Type of Report and Period Covered

13.

14. SUPPLEMENTARY NOTES

15. ABSTRACT *(A 200-word or less factual summary of most significant information. If document includes a significant bibliography ot literature survey, mention it here.)*

The radio wave propagation path between an earth station and a synchronous satellite is described by engineering-type formulas which consolidate all of the known external elements significant for system performance. This UHF/SHF consolidated model, adaptable for subsequent updating, includes state-of-the-art estimates of noise, attenuation, depolarization, and turbulence. The role of system geometry in signal depolarization is presented and the basis for the evaluation of linear versus circular polarization is developed. The conventional figures of merit are included; the determination of service fields (desired signal levels) and potential interference fields (undesired signal levels) are described. The application of the formulas and graphs given in the text are illustrated by numerical examples; their associated derivations are either referenced or covered in the Appendices.

16. Key words *(Alphabetical order, separated by semicolons)*
atmospheric attenuation; frequency allocation; depolarization; frequency sharing; interference fields; propagational effects; service fields; SHF; slant path; UHF.

17. AVAILABILITY STATEMENT

[X] UNLIMITED.

[ ] FOR OFFICIAL DISTRIBUTION.

18. Security Class *(This report)*
UNCLASSIFIED

19. Security Class *(This page)*
UNCLASSIFIED

20. Number of pages
92

21. Price: